



HAL
open science

Overview of naturally permeable fractured reservoirs in the central and southern Upper Rhine Graben: Insights from geothermal wells

Jeanne Vidal, Albert Genter

► To cite this version:

Jeanne Vidal, Albert Genter. Overview of naturally permeable fractured reservoirs in the central and southern Upper Rhine Graben: Insights from geothermal wells. *Geothermics*, 2018, 74, pp.57 - 73. 10.1016/j.geothermics.2018.02.003 . hal-01710805

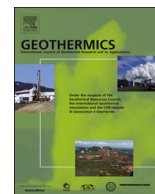
HAL Id: hal-01710805

<https://hal.science/hal-01710805>

Submitted on 16 Feb 2018

HAL is a multi-disciplinary open access archive for the deposit and dissemination of scientific research documents, whether they are published or not. The documents may come from teaching and research institutions in France or abroad, or from public or private research centers.

L'archive ouverte pluridisciplinaire **HAL**, est destinée au dépôt et à la diffusion de documents scientifiques de niveau recherche, publiés ou non, émanant des établissements d'enseignement et de recherche français ou étrangers, des laboratoires publics ou privés.



Overview of naturally permeable fractured reservoirs in the central and southern Upper Rhine Graben: Insights from geothermal wells

Jeanne Vidal^{a,*}, Albert Genter^b

^a IPGS, University of Strasbourg, 1 Rue Blessig, 67084, Strasbourg Cedex, France

^b ES-Géothermie, Bâtiment Belem, 5 Rue de Lisbonne, 67300, Schilligheim, France



ARTICLE INFO

Keywords:

Permeable fracture zones
Geothermal resources
Geothermal systems
Upper Rhine Graben

ABSTRACT

Since the 1980's, more than 15 geothermal wells have been drilled in the Upper Rhine Graben (URG), representing more than 60 km of drill length. Although some early concepts were related to purely matrix-porosity reservoirs or Hot Dry Rock systems, most projects in the URG are currently exploiting the geothermal resources that are trapped in fracture networks at the base of the sedimentary cover and in the granitic basement. Lessons-learned from the European EGS reference site at Soultz-sous-Forêts reveal highest natural permeability in the uppermost altered crystalline basement.

Here, we present a compilation of related information to examine a more general validity of this hypothesis for the central URG. In this respect, 15 geothermal wells were analyzed concerning their lithologies, temperature distribution with depth, and their hydraulic yields. Among others, permeable fractures in Triassic sediments were observed among others during drilling operations at Soultz-sous-Forêts, Rittershoffen, Cronenbourg (France), Landau, Insheim, Bruchsal and Brühl (Germany). The geothermal wells at Soultz-sous-Forêts, Rittershoffen (France), Landau and Insheim (Germany) also intersect well-connected fracture networks in the uppermost altered granitic basement. Permeable fractures are intersected to a depth of 5 km at Soultz-sous-Forêts (France) and Basel (Switzerland).

The compilation of geologic, hydraulic and thermal data of 15 geothermal wells shows permeability variation among the lithologies with the maximum observed at the top of the hydrothermally altered granite. This higher permeability is likely due to the intense fracture density in the fault core of the fracture zone and the large porous and altered damage zone which allow connection with the reservoir.

1. Introduction

The Upper Rhine Graben (URG) is a part of the European Cenozoic Rift System. This graben is characterized by a series of thermal anomalies that are widely interpreted as the signature of large-scale natural advection and convection on multi-scale fracture-controlled systems. These systems are associated with the nearly vertical faults that cross-cut both the deep-seated Triassic sediments and the Paleozoic crystalline basement rocks (Baillieux et al., 2013; Pribnow and Schellschmidt, 2000; Schellschmidt and Clauser, 1996). In both cases, fracture permeability exceeds matrix permeability. The overlying Tertiary sedimentary formations exhibit exceptionally high temperature gradients up to 100 °C/km and host hydrocarbons (Sittler, 1985). Over the past 35 years, geothermal projects have been developed in France, Germany and Switzerland to exploit deep geothermal energy.

Starting in Los Alamos (USA) and Cornwall (UK) in the 1970s, the exploitation of granitic systems was initially developed based on the

Hot Dry Rock (HDR) concept. The HDR concept was initiated to exploit the vast energy resources that reside as heat in the low-permeability rocks underlying most continental regions at depths accessible by wells (Schulte et al., 2010). The Soultz-sous-Forêts pilot project includes five deep wells intersecting the Triassic sediments and reaching the deep crystalline basement. Initially, HDR technology was used to artificially create a heat exchanger in the deep crystalline rocks. However, all wells exhibit at least one permeable natural fracture zone. The natural permeability of these fracture zones is often weak and needs to be enhanced to reach economically viable hydraulic yields. Thus, these reservoirs are often associated with Enhanced Geothermal System (EGS) technology, which involves engineering existing fractures to improve their low initial permeability (Ledru and Guillou-Frottier, 2010). At Soultz, the top basement is characterized by intense hydrothermal alteration (Traineau et al., 1992), where the flowrate is higher even if the temperature of the geothermal fluid is lower. It is well known that the natural reactivation potential and the susceptibility of fractured

* Corresponding author.

E-mail address: jeanne.vidal@es.fr (J. Vidal).

reservoirs to hydraulic stimulation is influenced by the lithology (Meixner et al., 2014) and in the particular case of the granitic basement, the degree, of hydrothermal alteration (Evans et al., 2005; Meller and Kohl, 2014). Recent geothermal projects are directly based on lessons learned from Soultz projects, where the initial natural permeability is highest in the fracture networks at sediment-basement interfaces (Schill et al., 2017). They are described as hydrothermal systems, and their economic exploitation does not require stimulation treatments.

In this paper, we investigate to what extent the observations at Soultz are systematic and representative of the central URG sediment-basement interface. To achieve this, 15 wells are compared with regard to their lithological differences and respective temperature and hydraulic indicators. These data are discussed in relation to observed fracture zones. Because hydraulic parameters are of critical economic relevance and are typically not publically available, temperature is used to infer heat transfer processes and, thus, hydraulic conditions in most cases. Following a presentation of fractured systems and hydrothermal circulation concepts in the URG, deep geothermal projects of the central and southern URG are discussed. The geothermal project of Soultz-sous-Forêts serves as a reference.

2. Structural evolution of the URG

The Upper Rhine Graben (URG) forms the central, most conspicuous segment of the ECRIS (Illies, 1965), which extends over a distance of more than 1000 km from the North Sea to the Mediterranean (Fig. 1). The NNE-trending URG, which is limited by the Rhenish Massif to the north and the Jura Mountains to the south, has a length of some 300 km and a width of 30–40 km. This geological setting will focus on the structural inheritance of the crystalline basement and the evolution of fractured system from Variscan to late Alpine.

The Variscan crystalline basement of the URG is characterized by three major tectonic terranes, oriented NE to NNE, from north to south, the Rhenohercynian, the Saxothuringian and the Moldanubian that present major lithological differences (Edel and Schulmann, 2009; Edel and Weber, 1995; Ziegler, 1990). They are intruded by carboniferous granitoid (340 Ma (Visean) and 270 Ma (Permian)) that exhibit a large petrological and geochemical diversity of crystalline rocks, which are related to a variety of active deep magmatic sources and different petrogenetic mechanisms (Altherr et al., 2000, 1999; Edel and Schulmann, 2009; Lagarde et al., 1992). These granitoids are emplaced following a NE to NNE direction according to main weakness zones such as collisional or shear zones. These inherited Hercynian NE to NNE-striking crustal weakness were reactivated to the URG formation under compressional stresses during Alpine and Pyrenean collisions (Dèzes et al., 2004; Edel et al., 2007; Illies, 1972, 1965; Schumacher, 2002; Villemin and Bergerat, 1987). Mesozoic platform sediments of Triassic (Buntsandstein, Muschelkalk and Keuper) and Jurassic (Lias and Dogger) times that results from eroded Variscan belt are also affected by structural evolution during Cenozoic rifting. (Villemin and Bergerat, 1987) and (Schumacher, 2002; Villemin and Bergerat, 1987) proposed a Cenozoic rifting of the URG divided into four brittle deformation phases, which were accompanied by different stress regimes from the late Eocene rifting to the late Miocene. The first phase (middle to late Eocene) was characterized by an N–S compressive regime. During the second phase (late Eocene to late Oligocene), major E–W extension resulted in the greatest rifting and the development of thick sedimentary sequences in the URG (Doebel, 1967). These events included two marine transgressions, which induced the deposition of the carbon-rich Pechelbronn layers and salt layers in the southern area of the graben, among others. During the early Miocene, the stress regime changed to an NE–SW-oriented compressive phase. This episode was characterized by the uplift of the upper mantle and crust, as suggested by the up-doming Moho and the beginning of volcanism at the Vogelsberg and Kaiserstuhl volcanos (Fuchs et al., 1987). The prevailing

stress regime in the URG from the late Miocene to the present has been a compressional regime with an NW–SE orientation, as observed over much of central Europe, which resulted in a left-lateral transcurrent motion (Bergerat, 1985; Illies and Greiner, 1979).

3. Thermal settings and fractured system

In the URG, the underground temperature distribution is spatially heterogeneous with a series of local anomalies with temperatures above 140 °C at 2 km Measured Depth (MD). Most of these values are concentrated on the western side of the URG, where the direction of the border fault rotates from N20°E to N45°E (Baillieux et al., 2014, 2013; Dezayes et al., 2015; Schellschmidt and Clauser, 1996). High resolution temperature data from wells reveal a spatial link between high temperature and local faults, such as the Soultz and Kutzenhausen faults, as well as the Ω -fault at Landau (Fig. 1) (Bächler et al., 2003; Baillieux et al., 2013; Benderitter et al., 1995; Pribnow and Clauser, 2000; Pribnow and Schellschmidt, 2000). Thus, these geothermal anomalies at the local scale are attributed to buoyancy-induced hydrothermal circulation in fractures within the crystalline basement and sandstones. For example, Fig. 2 shows the disturbance of isotherms resulting from geostatistical modelling (GeORG Team, 2013). The so-called ‘Soultz geothermal anomaly’ is one of the most important temperature anomalies and has been the subject of numerous studies. Hydrothermal convection may explain 75–85% of this anomaly (Baillieux et al., 2013), and the up-flow of thermal water occurs mainly along westward dipping normal faults (Baillieux et al., 2014). The radiogenic heat production due to the crystalline composition of the basement may explain the remaining 15–25% (Baillieux et al., 2013). The highest radiogenic productions are associated with hydrothermally altered zones. In the deep geothermal well GPK-1, radiogenic production determined from core samples ranges between 5.5–6.5 $\mu\text{W}/\text{m}^3$ for depths between 1400 and 1550 m MD (Rummel et al., 1988). Continuous logging of the deep geothermal well GPK2 revealed values up to 7 $\mu\text{W}/\text{m}^3$ between 3700 and 3800 m MD and at 5060 m MD in permeable zones (Grecksch et al., 2003; Pribnow, 2000).

All geothermal fluids collected in deep geothermal wells result from the mixing of primary marine brine (seawater evaporation at least up to the halite precipitation stage) and water of meteoric origins (Aquilina et al., 1997; Pauwels et al., 1993; Sanjuan et al., 2014, 2010). These fluids are of the Na-Cl type with high salinity values, approximately 100 g/L, and with pH values close to 5 (Sanjuan et al., 2016, 2014). Both fossil and present-day hydrothermal circulations in the fracture system have resulted in the strong dissolution of primary minerals, such as biotite and plagioclase, as observed in the granitic basement of Soultz, as well as the significant deposition of some altered minerals, such as clay minerals (smectite, illite, tosudite), calcite, secondary quartz and sulfides (Genter and Traineau, 1992). Circulation ages have been estimated from fracture filling dating at Soultz. Illites from fracture veins revealed ages from the Permian, Cretaceous, Miocene and earlier (Bartier et al., 2008; Schleicher et al., 2006). Hydrothermal circulations may have been linked to major volcanic events in the URG during the Permian (Lorenz and Nicholls, 1976), Cretaceous and Miocene (Illies, 1972). Mineralogical studies of assemblages in fracture fillings indicate a complex polyphase circulation system (Dubois et al., 2000; Smith et al., 1998).

4. History and structural setting of the geothermal wells

Table 1 and Figs. 3 and 4 show the geothermal wells used in this study, which are located in the central and southern URG, as well as their structural setting in chronologic order.

Triassic sediments were assessed in the early 80 s with the objective of exploiting the Mesozoic aquifers. In this context, the geothermal well GCR-1 was drilled in 1984 at Cronenbourg (Alsace, France) into the sandstones of the Buntsandstein (Lower Triassic age) (Housse, 1984).

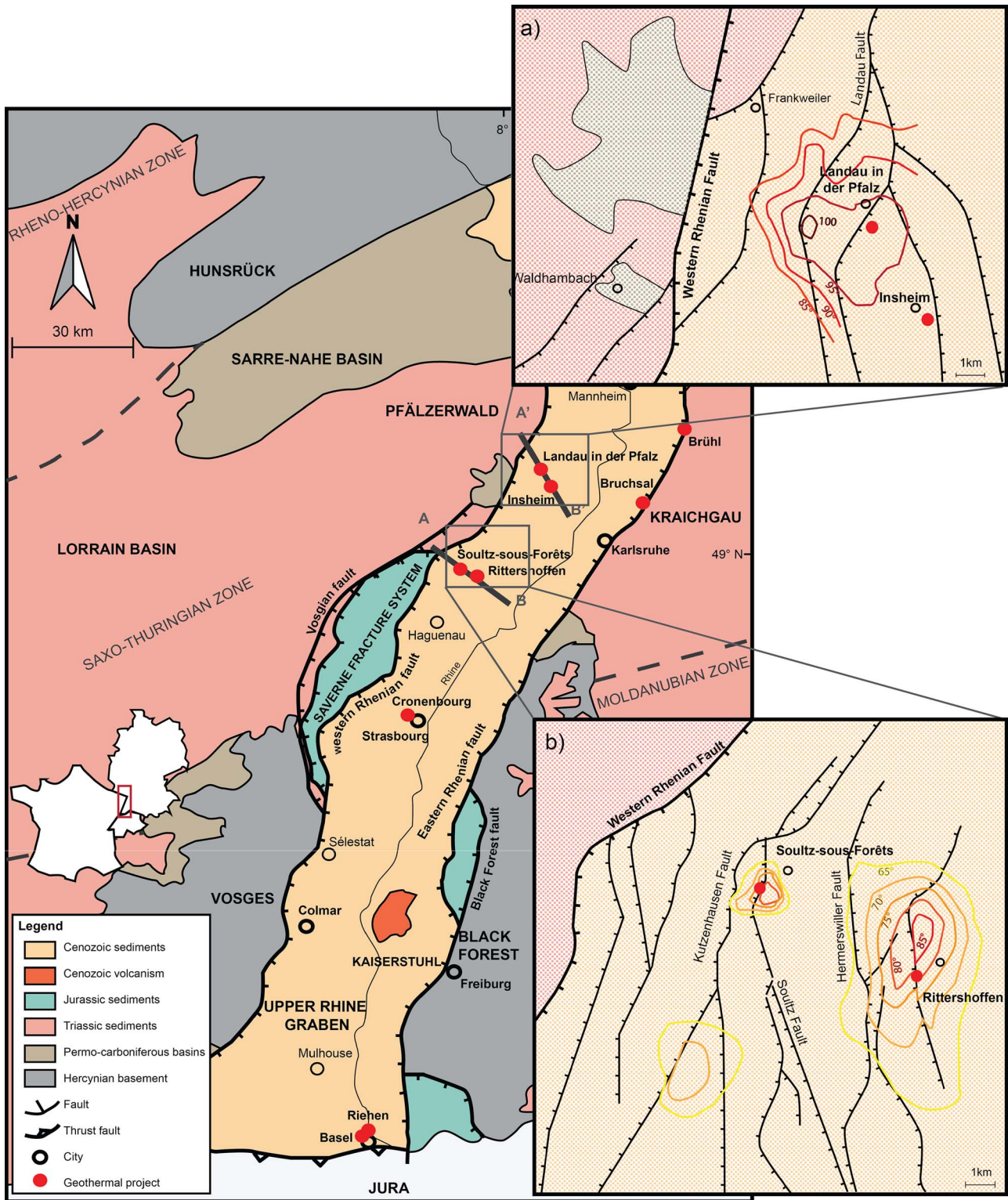


Fig. 1. a) Simplified geological map of the Upper Rhine Graben and surrounding low mountain ranges, as well as basins including structural settings of selected high temperature areas of b) Soultz-sous-Forêts and Rittershoffen (Baillieux et al., 2014), and c) Landau and Insheim (Eisbacher and Fielitz, 2010; “Geoportail of EU-Project GeORG – INTERREG IV Upper Rhine,” 2012). AB and A’B’ represent cross-sections that are detailed in Fig. 2.

The well was drilled vertically into a tilted block that was divided by a normal fault that strikes NE-SW and dips westward. The productivity of the well was too low to warrant an economically viable geothermal loop. Hydraulic testing showed that compared to the matrix, the natural permeability was higher in localized fracture zones. Accordingly, the matrix permeability concept was shown to be ineffective for deep

geothermal exploitation in the URG.

In 1983 at Bruchsal (Rhine Palatinate, Germany), two geothermal wells named GB-1 and GB-2 were drilled to exploit the geothermal resources of the Buntsandstein and Permian sandstones (Herzberger et al., 2010). They were drilled nearly vertically in an accommodation zone with a high density of normal faults striking N-S to N10°E and

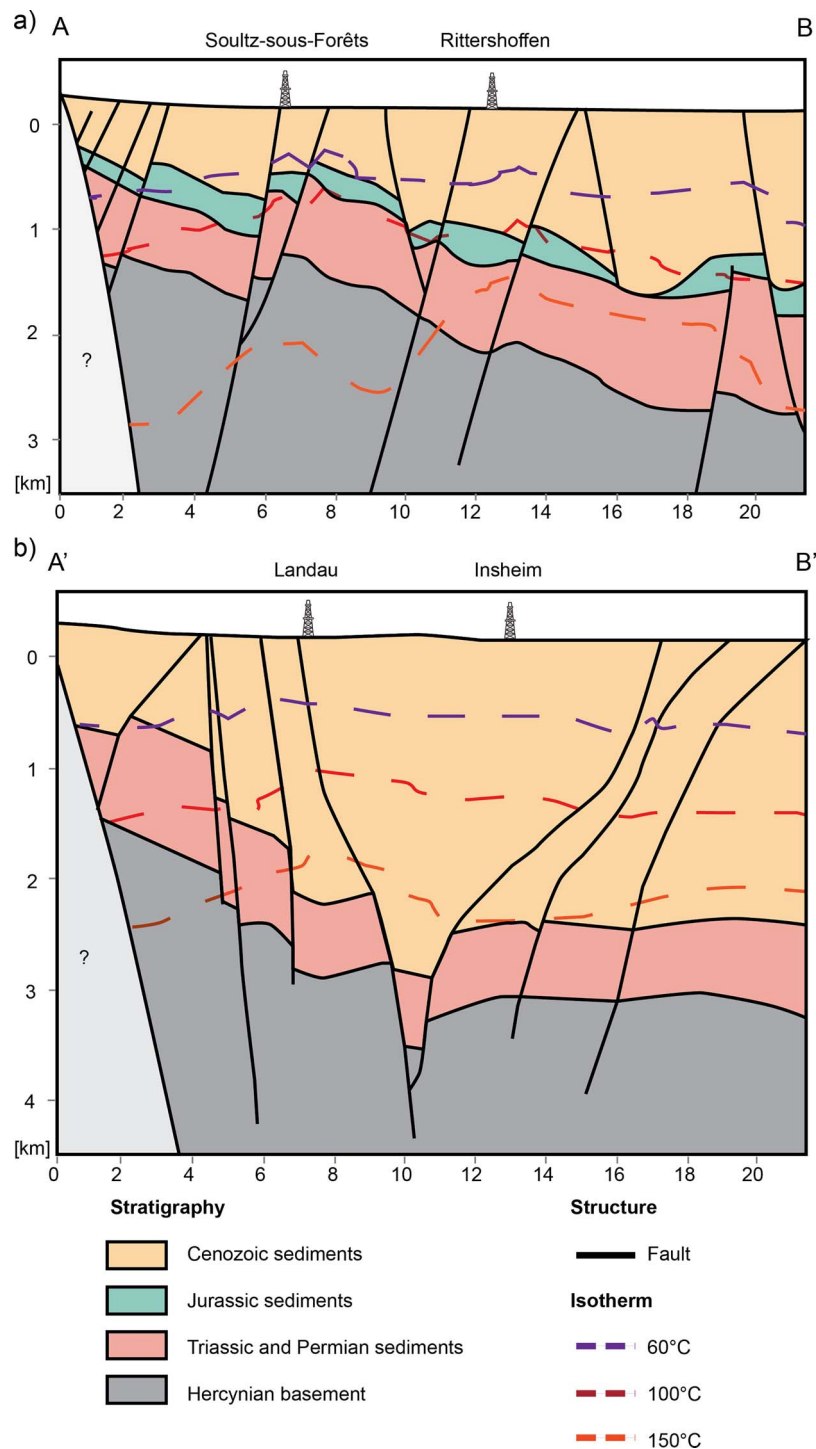


Fig. 2. Simplified geological cross sections and isotherms obtained from geostatistical modelling across Sultz and Rittershoffen geothermal fields (AB in Fig. 1) and across Landau and Insheim geothermal fields (A'B' in Fig. 1) modified after (“Geoportal of EU-Project GeORG – INTERREG IV Upper Rhine,” 2012).

dipping westward (Meixner et al., 2016). They intersect two different tilted blocks separated by a NW-SE striking fault.

The second set of approaches was mainly temperature-driven. In this framework, the project at Sultz-sous-Forêts (Alsace, France) is used as reference. It was the first project in the URG to create a deep granitic reservoir based on the Hot Dry Rock (HDR) concept (Gérard and Kappelmeyer, 1987). To produce electricity without the use of binary plant technology, the minimum required temperature was 200 °C. At a geothermal gradient of about 100 °C/km, the exploration well GPK-1 was drilled vertically down to 2000 m MD in 1987 in a horst

that is bordered by the Sultz fault system (Cautru, 1988; Herbrich, 1988). At the top of the basement, the main branch of the normal fault strikes N170°E and dips westward (Sausse et al., 2010). This well revealed brine at a temperature of up to 140 °C (Herbrich, 1988). It circulates through hydrothermally altered fracture zones at the top of the basement and thus reduces the geothermal gradient to about 10 °C/km. Aiming for “dry” rocks at higher temperatures, the well was deepened and reached a temperature of about 150 °C at 3500 m MD and an intermediate deep fracture network (Aquilina et al., 1993). An intermediate reservoir was developed at about 3600 m MD with a second

Table 1
 Properties of geothermal wells in the URG at Cronenbourg (Housse, 1984; Pauwels et al., 1993), at Bruchsal (Herzberger et al., 2010; Meixner et al., 2016; Sanjuan et al., 2016), at Soultz-sous-Forêts (Baria et al., 1995; Dezayes et al., 2005b; Genter et al., 2010; Hettkamp et al., 2007, 2004; Jung, 1992; Jung and Weidler, 2000), at Basel (Häring et al., 2008; Ladner and Häring, 2009), at Landau (Sanjuan et al., 2016; Schindler et al., 2013; Baumgärtner and Lerch, 2013; Sanjuan et al., 2017; Sanjuan et al., 2016) and at Brühl (Melchert et al., 2013; Sanjuan et al., 2016).

Name	Location	Year of drilling	Trajectory	Drilled Length (m MD)	Top of the Open-Hole (m MD)	Lithology of the Open-Hole	Initial hydraulic yield/ Post-stimulation (L/s/bar)	Stimulation	T _{Bottom} (°C)	pH	TDS (g/L)
GCR-1	Cronenbourg	1980	Sub-Vertical	2870	2664	Sandstones (Buntsandstein)	0.12	–	140	6.70	104
GB-1	Bruchsal	1983	Sub-Vertical	1932	1573	Sandstones (Buntsandstein)	–	–	120	5.06	121
GB-2	Bruchsal	1984	Sub-Vertical	2542	2350	Sandstones (Buntsandstein)	0.7	–	134	–	–
GPK-1	Soultz-sous-Forêts	1987 Deepening in 1992	Sub-Vertical	3590	2850	Hydrothermally Altered Granite (Carboniferous)	upper granitic reservoir 0.09 intermediate granitic reservoir 0.05	Hydraulic stimulation	160	–	–
GPK-2	Soultz-sous-Forêts	1994 Deepening in 1999	Sub-Vertical and deviated to the NW	5060	4440	Granite (Carboniferous)	intermediate granitic reservoir 1.6 deep granitic reservoir 0.02	Hydraulic and chemical stimulation	200	4.98	100
GPK-3	Soultz-sous-Forêts	2002	Sub-Vertical and highly deviated to the South	5110	4592	Granite (Carboniferous)	deep granitic reservoir 0.2	Hydraulic and chemical stimulation	200	–	–
GPK-4	Soultz-sous-Forêts	2003	Sub-Vertical and highly deviated to the South	5270	4767	Granite (Carboniferous)	deep granitic reservoir 0.4 0.01 0.5	Hydraulic and chemical stimulation	200	–	–
BS-1	Basel	2006	Sub-Vertical	5000	4629	Granite (Carboniferous)	2.5×10^{-3}	Hydraulic stimulation	190	–	–
Gt La-1	Landau	2005	33°W	3300	2100	Granite (Carboniferous)	–	–	160	4.96	106
Gt La-2	Landau	2006	25°E	3170	2200	Granite (Carboniferous)	0.25	Hydraulic and chemical stimulation	170	–	–
GTL-1	Insheim	2008	Highly deviated to SE	3850	3620	Sandstones (Permian)	> 1	Hydraulic stimulation and drilling of a sidetrack	165	5.23	107
GTL-2	Insheim	2009	Highly deviated to NE	3850	2980	Granite (Carboniferous) Sandstones Granite (Carboniferous)	–	–	–	–	–
GRT-1	Rittershoffen	2012	Sub-Vertical	2580	1925	Sandstones (Buntsandstein) Granite (Carboniferous)	0.5	Thermal, hydraulic and chemical stimulation	160	6.27	101
GRT-2	Rittershoffen	2014	37° to the North	3200	2120	Hydrothermally Altered Granite (Carboniferous) Sandstones (Buntsandstein) Hydrothermally Altered Granite (Carboniferous)	2.5 3.5	–	180	–	–
GT-1	Brühl		30°SE	2542	3155	Granite (Carboniferous) Sandstones (Buntsandstein)	3.5	–	170	–	100

Bold values are for post-stimulation.

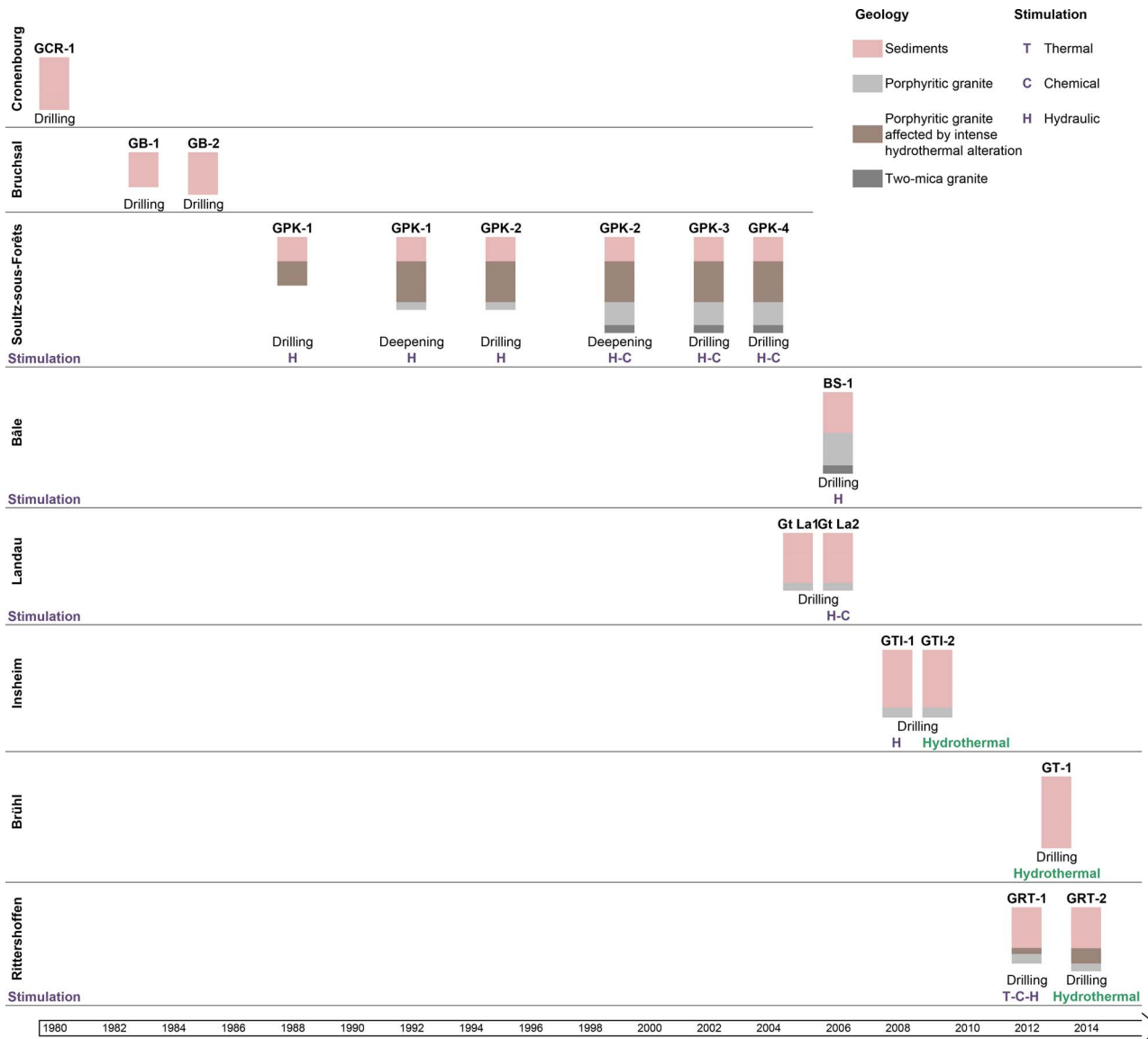


Fig. 3. Chronology of the deep geothermal projects and their associated wells in the URG. For each well, lithologies of open-holes are represented in depths along the borehole and stimulation treatments are detailed.

well, GPK-2, in 1992 (Dezayes et al., 2005b; Genter and Tenzer, 1995). The initial goal was to monitor the micro-seismicity during the creation of the heat exchanger to ensure the effectiveness of hydraulic operations. The GPK-2 well was deepened to 5000 m MD and two wells, GPK-3 and GPK-4, were drilled down to 5000 m True Vertical Depth (TVD) between 2000 and 2004 (Baumgärtner et al., 2000; Dezayes et al., 2005a,b, 2003). The deep granitic reservoir shows comparatively lower fracture density and lower hydraulic yield prior to stimulation. At Soultz, however, all five wells exhibit at least one permeable fracture zone, and the natural fracture network acts as a natural heat exchanger. Its natural permeability may be too weak for industrial exploitation. Note that at Soultz, wells were drilled parallel to the maximum horizontal stress and the main fault zones. The presence of fracture zones were not adequately taken into consideration before drilling and stimulation operations began. EGS technology was used in all wells with improvement factors of 30–50, but natural ambient test conditions at the sediment-basement level were never achieved in the deep reservoirs (Nami et al., 2008; Portier et al., 2009; Schill et al., 2017).

Following the temperature-driven concept of Soultz, the BS-1 well was drilled in 2006 at Basel (Switzerland) for the Deep Heat Mining project (Häring et al., 2008). The deep granitic section of the well

revealed a very low initial hydraulic yield and was hydraulically stimulated. Induced seismic events with magnitudes up to $M = 3.4$ interrupted the project (Häring et al., 2008).

The following projects developed in the URG were based on lessons learned from Soultz and EGS technology, and targeted the sediment-basement interface and not the deep granitic basement.

In 2005, the geothermal doublets Gt La1 and Gt La2 were drilled at Landau (Baden-Württemberg, Germany). For the first time in the URG, the wells were deviated 33° westward and 25° eastward, respectively (Baumgärtner, 2007). They targeted local normal faults within a horst/graben system that strike N-S and dip eastward (Schad, 1962). The geothermal reservoir at Landau was developed using a multi-reservoir concept (Triassic and Permian sandstones – altered granite) (Hettkamp et al., 2007).

In line with the concept of cross-cutting fault zones, the geothermal doublets GTI-1 and GTI-2 were drilled at Insheim (Baden-Württemberg, Germany) in 2008. The geothermal target was a normal fault oriented N-S that dips westward in a horst/graben system (Baumgärtner et al., 2013). Both wells intersected this fault with a deviated trajectory to the NW and SE (Baumgärtner et al., 2013). The geothermal reservoir at Insheim was also developed on a multi-reservoir concept (Muschelkalk

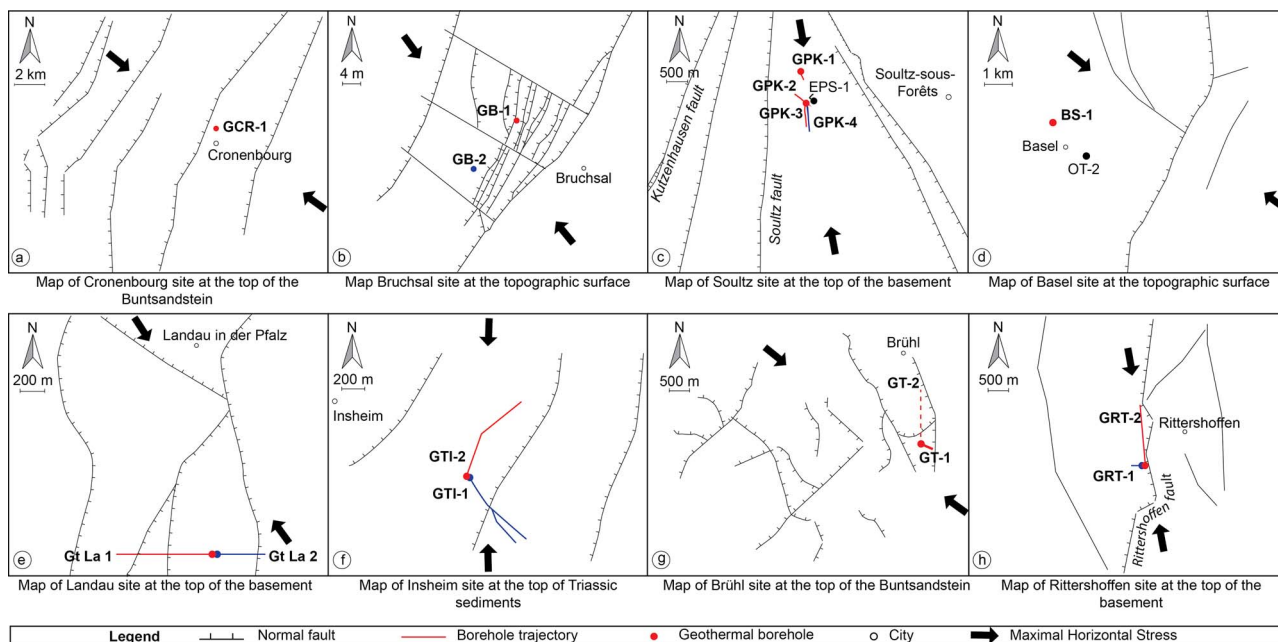


Fig. 4. Maps of geothermal sites with fault traces and well trajectories located a) at the top of the Buntsandstein at Cronenbourg (Housse, 1984), b) at the topographic surface at Bruchsal (Meixner et al., 2016), c) at the top of the basement at Soultz-sous-Forêts (Sausse et al., 2010), d) at the topographic surface at Basel (Meixner et al., 2016), e) at the top of the basement at Landau (Rueter, 2010), f) at the top of the Triassic sediments at Insheim (Baumgärtner et al., 2013), g) at the top of the Buntsandstein at Brühl (Lotz, 2013), and h) at the top of the basement at Rittershoffen (Baujard et al., 2017). Maximum horizontal stress in open-holes are oriented N142°E at Bruchsal (Meixner et al., 2014), N170°E at Soultz (Valley, 2007), NNW-SSE at Landau (Ritter et al., 2014), N-S at Insheim (Baumgärtner et al., 2013), N140°E at Brühl (Reinecker et al., 2014) and N170°E at Rittershoffen (Hehn et al., 2016). Regional maximum horizontal stress is indicated for Cronenbourg and Basel.

– Rotliegendes – altered granite) (Baumgärtner and Lerch, 2013). A sidetrack and a hydraulic stimulation were achieved within the GTI-1 well to reach the expected flowrate, whereas the GT-2 well was hydraulically and chemically stimulated (Schindler et al., 2010).

At Brühl (Rhine Palatinate, Germany), the geothermal GT-1 well was drilled down to the Buntsandstein formation in 2013 (Lotz, 2013). The well is deviated by 30° to the SE and intersects a normal fault that is oriented N170°E to N-S and dips westward (Lotz, 2013; Reinecker et al., 2014).

At Rittershoffen (Alsace, France), a geothermal doublet was installed between 2012 and 2014, including GRT-1 and GRT-2 (Baujard et al., 2017). The wells targeted the Rittershoffen normal fault that borders a local graben system (Baujard et al., 2017). This fault strikes N10°W to N10°E and dips westward. GRT-1 intersects the fault vertically and GRT-2 is deviated 37° to the north. The GRT-1 well stimulated based on a combined thermal-chemical-hydraulic stimulation, including environmentally friendly solutions (Recalde Lummer et al., 2014; Recalde Lummer et al., 2014; Recalde Lummer et al., 2014; Recalde Lummer et al., 2014), packer utilization to isolate treated zones, and low-pressure hydraulic injections (Recalde Lummer et al., 2014; Vidal et al., 2016b).

5. The reference geothermal site of Soultz-sous-Forêts

In this section, geologic, hydraulic and thermal properties of geothermal reservoirs at Soultz are discussed. They provide a reference for comparison with the data from the geothermal wells listed in Table 1 in Sections 6 and 7.

At Soultz, EGS developments consist of crystalline basement rock and extend over three reservoir levels: 2000 m TVD (upper reservoir), 3500 m TVD (intermediate reservoir), and 5000 m TVD (deep reservoir). About 15 major hydraulic and chemical stimulations were carried out to improve reservoir conditions at those different levels (Schill et al., 2017). Potential shallow reservoirs from 1200 m to 1400 m TVD in the Triassic sediments and the altered top of the granitic basement (reddish granitic reservoir) have shown some occurrences of

partial or total mud losses related to fracture zones in the sediments during drilling operations (Vidal et al., 2015). This potential reservoir was never hydraulically tested or stimulated. In the intermediate and deep reservoirs, long-term productivity was demonstrated during nine periods in 1997, 2005 and between 2008 and 2013. The deepest reservoir was developed to ensure electricity production.

5.1. Fracture network and hydraulic yields of the reservoirs

In the following section, we discuss the fracture network and hydraulic yields from the deep to the shallow granitic, the altered top granitic and the sedimentary potential reservoir rocks (Table 1). The deep granitic basement of Soultz-sous-Forêts is accessed through the open-hole sections from 4500 to 5230 m MD. It consists of a grey fine-grained two-mica granite (327 ± 7 Ma) (Cocherie et al., 2004; Stussi et al., 2002). The matrix porosity of the two-mica granite is approximately 0.5% (Géraud et al., 2010). The fracture density in GPK-3 and GPK-4 is approximately 0.8–0.9 fract/m below 4500 m MD and decreases to 0.25 fract/m below 5080 m MD (Valley, 2007). The fractures mainly strike N-S and dip to the west. A major fault zone intersected the GPK-3 well between 4755 and 4780 m MD and controls 70% of the flowrate in the well (Dezayes et al., 2010b). This zone consists of 7 individual fractures with a cumulative altered granite thickness of 15 m. The deep granitic reservoir showed an initial injectivity index of 1 × 10–2 L/s/bar in GPK-4 and 2 × 10–2 L/s/bar in GPK-2. Undisturbed conditions in GPK-3 were not determined (Schill et al., 2017). After hydraulic and chemical stimulation, hydraulic yields range from approximately 0.4 L/s/bar in GPK-3 to approximately 0.5 L/s/bar in GPK-4 and approximately 1 L/s/bar in GPK-2 (Hettkamp et al., 2004; Nami et al., 2008; Portier et al., 2009; Schill et al., 2017). Maximum hydraulic yields of up to 2 L/s/bar were observed in 2011 after several years of operation. Note that for these values, contributions from the intermediate reservoir due to casing leakage cannot be excluded.

In the intermediate reservoir, a gray porphyritic monzogranite (334 ± 4 Ma) was encountered above a fine-grained two mica granite (Cocherie et al., 2004; Stussi et al., 2002). In GPK-3 and GPK-4, the

fracture density is approximately 0.5–0.6 fract/m according to acoustic image logs in this section (Valley, 2007). In GPK-2 and GPK-1, the fracture density is approximately 0.4–0.5 fract/m between 2100 and 3500 m MD according to acoustic image logs (Genter et al., 1997a). This value increases up to 1.3 fract/m between 1600 and 2100 m MD in the upper reservoir. According to EPS-1 cores, the density is around 0.8 fract/m within the same depth section. The fractures are oriented N-S to NNE-SSW with a steep dip ($> 60^\circ$) eastward or westward. In this section, the natural permeability is intimately linked to hydrothermally altered fracture zones (HAFZ) affecting the monzogranite. These zones consist of a highly fractured fault core, which is surrounded by an altered, porous and fractured damage zone (Genter et al., 2000). The damage zone is characterized by strong alteration with the leaching of primary minerals and the precipitation of secondary minerals (quartz, clays, carbonates, hematite, and sulfides) (Genter and Traineau, 1996). These minerals are related to the early pervasive alteration stage that affected the granite on a large scale and the later vein alteration stage that was controlled by the fracture network. Quartz, illite and carbonates are located within the main fracture zones, and barite, galena and pyrite occur sporadically. Chlorites, epidote and carbonates are found in tiny natural fractures in massive granite. Quartz veins observed in core samples or in cuttings correspond to a localized decrease in gamma rays (2160 m MD in Fig. 5a). Quartz veins, which are mainly localized into the fault core, correspond to the precipitation of silica-rich fluids derived from the dissolution of primary silicate minerals during vein alteration. They are associated with high reflectivity in the dark mottled zone in acoustic images (Fig. 5a). In EPS-1, the acoustic image presents a low quality. The surrounded damage zone is a highly hydrothermalized and clay-rich zone associated with an increase of the gamma rays (Fig. 5a). The porosity of the damage zone is higher than in the fault core (2163–2164 m MD in Fig. 5a). The highest porosity of this fracture zone is approximately 25% in the damage zone (Ledéseret et al., 1999). The main permeable fracture zones were intersected between 2155 and 2190 m MD in EPS-1, between 1810 and 1825 m MD in GPK-1 and between 1970 and 2110 m MD in GPK-2 (Dezayes et al., 2010b). These regions exhibit more than 100 fractures with a cumulative fracture zone thickness of 10–15 m. The major permeable drains are 10 m thick (Genter et al., 1997b). The pre-stimulation injectivity in GPK-1 in the upper reservoir varies between 9×10^{-2} L/s/bar (Jung, 1992) and is undetermined at undisturbed conditions in GPK-2. In the intermediate reservoir, GPK-1 and GPK-2 show initial hydraulic yields of 5×10^{-2} and 3×10^{-2} L/s/bar, respectively, that are enhanced to approximately $> 1.6 \times 10^{-1}$ L/s/bar after hydraulic stimulation (Jung and Weidler, 2000; Schill et al., 2017). Hydraulic fracture stimulation, or hydro-shearing, does not require that proppants inside the stimulated fractures maintain a higher resulting permeability. Hydraulic stimulation causes an irreversible increase in the permeability by releasing the shear stress operating in the vicinity of the stimulated fractures. The effectiveness of hydro-shearing, which induces micro-seismicity activity, is linked to the initial low planarity and high roughness of the natural fracture surfaces. The post-stimulation behavior of reactivated fractures allows a self-propping and a permeability increase, which is sustainable during exploitation. During hydraulic stimulation, induced seismicity is less intense in the intermediate granitic reservoir than in the deep reservoir (Cuenot et al., 2008), likely due to the presence of secondary clay minerals (Meller and Kohl, 2014).

The top of the granitic basement consists of a 150 m-thick reddish granitic layer, which was observed in all geothermal wells. This section was affected by a paleo-weathering alteration event because of paleo-emersion during the Permian. The bulk porosity in this section is between 2% and 7% (Géraud et al., 2010). Primary magnetic and ferromagnetic minerals, such as magnetite and biotite, were leached, decreasing the magnetic content as measured on a continuous Soultz core (Rummel, 1992). From a structural perspective, sub-horizontal joints that were most likely related to the granite's uplift during the Permian were superimposed by sub-vertical fractures. The fracture density is 9

fract/m (Genter et al., 1997a). Sub-horizontal joints strike N120°E and dip 10°–40°S. Despite the high fracture density and high porosity of this granitic formation, no permeability was observed during drilling operations. This lack of permeability was confirmed by hydraulic tests that were performed in GPK-1 (Herbrich, 1988). The fractures were mainly sealed by hematite, carbonates and clays (Genter and Traineau, 1996).

The transition between the granitic basement and the sedimentary cover is located at a depth of approximately 1400 m. The base of the sedimentary cover consists of Permian coarse-grained to micro-conglomeratic sandstones that are 10 m thick. Annweiler sandstones are the first sandstones from Triassic formations (Vernoux et al., 1995). Thus, the 50 m-thick formation is argillaceous red sandstone. This formation shows an erosive contact with the Vosgian sandstones, which consist of typical medium-grained to conglomeratic continental sandstones with clay formations. After the so-called Intermediate beds, which are 40-m-thick large-grained sandstones, the 10-m-thick Voltzia sandstones include fine-grained sandstones with interbedded clays that overlie the Buntsandstein formation. The porosity reaches 20% in the Vosgian sandstones and approximately 10% in the intermediate beds and in the Annweiler sandstones (Griffiths et al., 2016; Haffen et al., 2013; Vernoux et al., 1995). The fracture system is conjugated and strikes N170°E with a dip of 75°W or 75°E (Vernoux et al., 1995). The fracture density is 0.8 fract/m, and the fractures are mainly filled by barite and calcite. Galena, pyrite, quartz and hematite were also observed as fracture fillings alongside organic materials and oil impregnation. The major permeable fault zone intersects EPS-1 between 1170–1215 m MD. This zone consists of more than 50 fractures with a maximum individual thickness of 5 cm. The fault zone was also intersected at 1220 m MD in GPK-1 (Dezayes et al., 2010b) and at 1265 m MD in a peripheral Soultz well called 4550. The intersected fault zone produces 30 m³/h with a natural post-drilling productivity estimated to be 1 L/s/bar (Degouy et al., 1992). This value is estimated from a Drill Stem Test that is not strictly representative of the hydraulic yield of a geothermal well.

The Middle Triassic formation is called Muschelkalk and is 150 m thick. This formation consists of fossil-rich sandstones at the base, marly dolomites that were invaded by anhydrite, and massive limestones at the top (Aichholzer et al., 2015). A permeable fracture zone intersects at approximately 950 m MD in the Middle Muschelkalk of the EPS-1 well, approximately 1000 m MD in GPK-1, and approximately 950 m MD in GPK-2, -3, and -4 (Vidal et al., 2015). EPS-1 core samples indicate the presence of hydraulic breccia at approximately 950 m MD in this layer.

5.2. Thermal profiles in Soultz wells

The typical thermal profile in the URG can be divided into two major sections (Fig. 6). The uppermost region consists of sedimentary formations from the Tertiary and Mesozoic (Jurassic and Upper Triassic) and features a high geothermal gradient of up to 100 °C/km, which indicates a conductive heat transport mechanism (Pribnow and Schellschmidt, 2000). These geological layers act as a cap rock, i.e., an impermeable layer that insulates an active hydrothermal system below. The latter is associated with a low geothermal gradient of about 10 °C/km in the hydrothermally altered granitic basement (Fig. 6). In the Muschelkalk limestones, Buntsandstein and Permian sandstones, a zone of smooth transition between conduction and convection is observed. The deep granitic basement is associated with a mean geothermal gradient of 30 °C/km indicating a conduction process (Fig. 6). The thermal profiles are locally disturbed by fracture zones. Negative anomalies on the temperature logs are the thermal signature of HAFZ that were cooled by drilling, massive hydraulic injections and the circulation of cold water (Genter et al., 2010). For example, in GPK-3 and GPK-2, the permeable fracture zone between 4755–4780 and between 1970–2110 m MD are associated with a local negative temperature

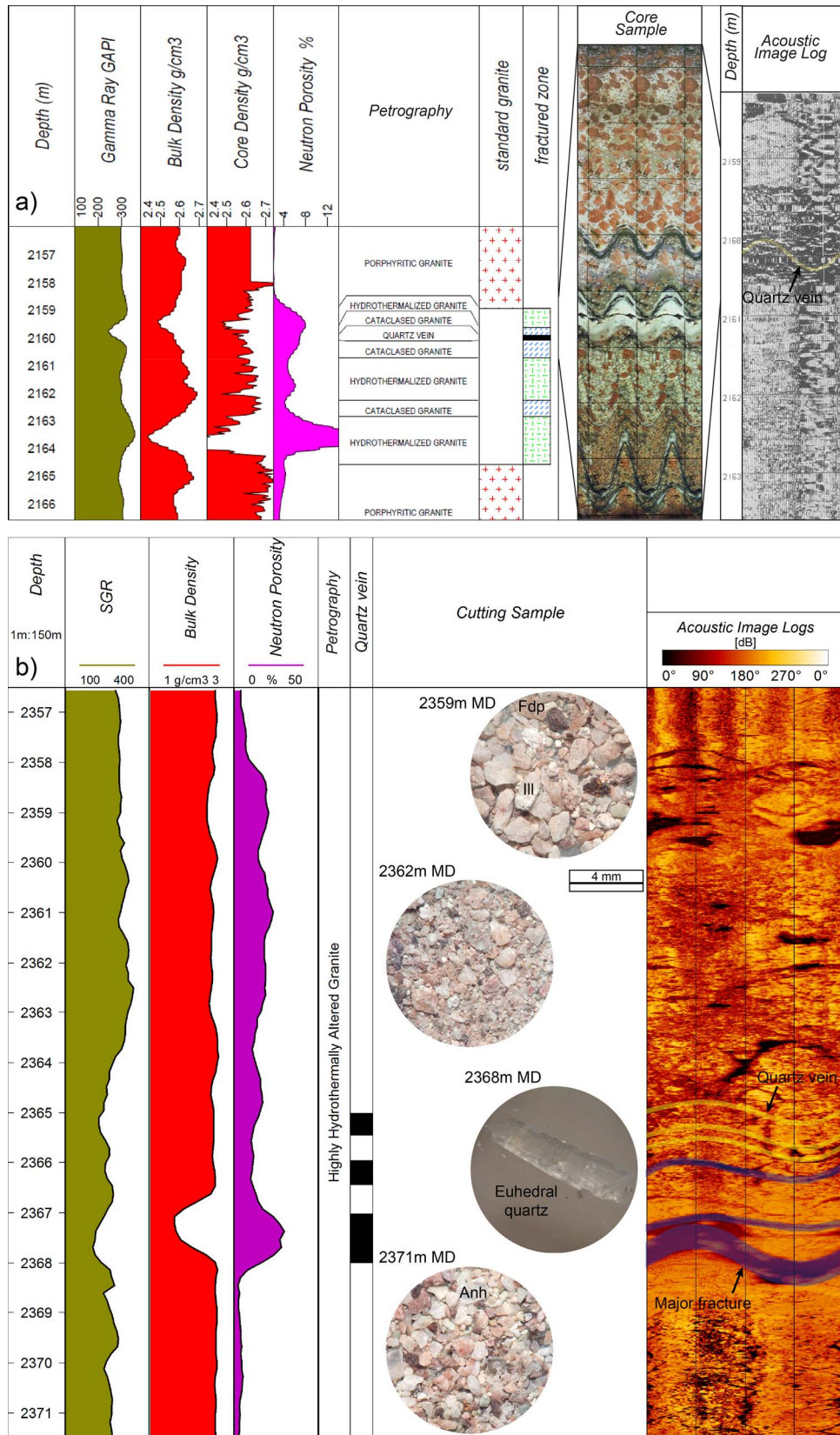


Fig. 5. Composite logs of major permeable fracture zones a) in EPS-1 well at Sultz-sous-Forêts and b) in GRT-1 well in Rittershoffen. Well logs in the EPS-1 well are from (Dezayes et al., 2010a). The hydrothermal alteration is linked to the fracture and thus the interfaces between levels of alteration are highly dipping.

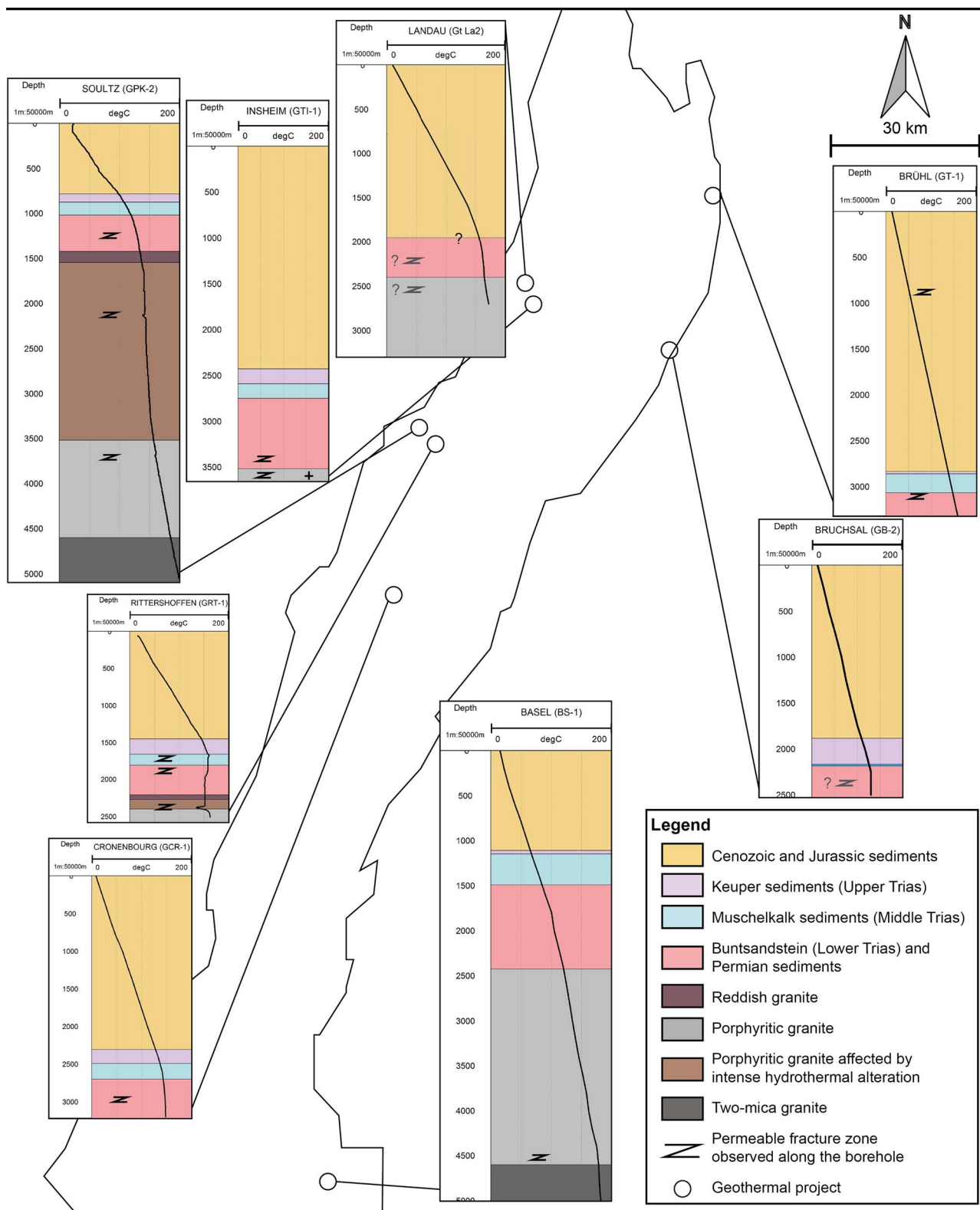


Fig. 6. Thermal profiles that are associated with the geology and permeable fracture zones in geothermal wells in central and southern URG. The depths are given in units of measured depth. At Sultz, the thermal profile was acquired at the thermal equilibrium in GPK-2 in January 1999 (Genter et al., 2010). At Cronenbourg, and the thermal profile in GCR-1 was acquired at the thermal equilibrium in December 1981 (Housse, 1984). The deepest part below 2700 m MD is extrapolated. At Bruchsal, the thermal profile in GB-2 was acquired at the thermal equilibrium (Herzberger et al., 2010). At Basel, the deepest part of the geothermal profile in BS-1 is approximated (Ladner and Häring, 2009). At Landau, the thermal profile in Gt La2 is extrapolated (Schindler et al., 2010). At Insheim, the thermal profile is not published and only the equilibrium bottom hole temperature is published (Baumgärtner and Lerch, 2013). At Rittershoffen, the thermal profile was acquired at equilibrium in GRT-1 in July 2015 (Baujard et al., 2017). At Brühl, the thermal profile was acquired in September 2013 (Melchert et al., 2013).

anomalies. However, permeable fracture zones observed in the Muschelkalk limestones and Buntsandstein sandstones are not associated with thermal anomalies (Fig. 6).

The temperature in the hydrothermally altered granitic reservoir is between 160 °C and 170 °C. The bottom hole temperature reached at 5 km depth is 200 °C (Fig. 6).

6. Geological and hydraulic yields of geothermal reservoirs in central and southern URG

In the following section, the central and southern URG reservoirs are grouped according to their lithology. In Figs. 6 and 7, geological and hydraulic properties are compared to each other and to the respective Soultz reference reservoir.

6.1. Two-mica granite reservoir

Except for the deep reservoir of the reference site at Soultz, only the geothermal well BS-1 at Basel reaches the deep two-mica granite at a depth of > 4600 m. It is composed of hornblende-biotite-rich and quartz-poor granitoid rocks (Käser et al., 2007). The fractures strike NW-SE to NNW-SSE with steep dips, and the fracture density is approximately 0.2–0.3 fract/m. Two cataclastic fracture zones intersect BS-1 at 4700 and 4835 m MD, and the cuttings exhibit significant amounts of anhydrite and illite. Their initial hydraulic yield is very low, with an injectivity index of 2.5×10^{-3} L/s/bar, which is increased by two orders of magnitude directly after hydraulic stimulation (Ladner and Häring, 2009).

6.2. Hydrothermally altered granitic reservoir

At Basel, a hornblende-biotite monzogranite overlies the two-mica granite and is characterized by a fracture density of 0.95 fract/m (Käser et al., 2007). The fracture orientation is the same as in the deepest section. No natural permeable fracture zone was observed in this section of BS-1.

Undistinguished porphyritic granite has been reported from the geothermal sites of Landau and Insheim. At Landau, granite was encountered at approximately 2400 m MD (Schindler et al., 2010). Similarity to the Soultz and Rittershoffen, the granitic basement can be expected because all three belong to the Saxothuringian unit. Water-bearing fractures likely control the flowrate in the granitic reservoir according to the shape of the thermal profile (Fig. 6) (Hettkamp et al., 2007; Schindler et al., 2010). The injection well Gt La2 showed an injectivity of approximately 0.25 L/s/bar before stimulation and > 1 L/s/bar after hydraulic and chemical stimulation (Schindler et al., 2010). The initial productivity of Gt La1 is not published.

At Insheim, granite was encountered at approximately 3500 m MD (Baumgärtner et al., 2013). Permeable fracture zones intersect GTI-1 and GTI-2 (Baumgärtner et al., 2013). The productivity in GTI-1 was 0.9 L/s/bar before hydraulic stimulation and increased after side-track operations (Baumgärtner et al., 2013). The initial hydraulic yield of GTI-2 is not published.

The bottom holes of GRT-1 and GRT-2 at Rittershoffen consist of porphyritic granite with different degrees of hydrothermal alteration, which is similar to those at Soultz (Vidal et al., 2017b). From the top of the granitic basement to 2400 m MD, the porphyritic granite is affected by an intense hydrothermal alteration. The fracture density is around 0.6–1 fract/m at the top and decreases with depth to 0.3 fract/m (Vidal et al., 2016a). The fractures strike N165°E to N-S and dip 65°W or E. The GRT-1 well exhibits one major permeable fault zone that intersects between 2325 and 2370 m MD (Vidal et al., 2016b). It controls 70% of the flowrate and is associated with a negative temperature anomaly (Baujard et al., 2017). The main permeable fracture is 24 cm thick at 2368 m MD and is surrounded by quartz veins. These quartz veins are associated with localized decreases of gamma rays and a high

reflectivity in acoustic images (Fig. 5b). Acoustic images present very good quality in GRT-1, but only cutting samples are available, and the petrographic and structural interpretations are less accurate than when using core samples. The damage zone above consists of 50 fractures with a cumulative individual thickness that reaches 25 cm. It is associated with a high porosity of up to 30% due to the dissolution of primary minerals. The increase in gamma rays associated with this zone indicates that the secondary illitization of the zone is also observed in cutting samples. Mineralogical investigations indicated that the first hundreds of meters of the granitic reservoir are illitized because of hydrothermal alteration (Vidal et al., 2017a). The GRT-2 well exhibits four permeable fracture zones in this section, associated with temperature anomalies (Baujard et al., 2017). The main fault zone intersects at 2765 and 2800 m MD (Vidal et al., 2017a). This zone consists of 30 fractures with a cumulative individual thickness that reaches 17 cm. The initial injectivity was < 0.5 L/s/bar in GRT-1 and 2.5 L/s/bar after thermal, chemical and hydraulic stimulations, and the initial productivity was around 3.5 L/s/bar in GRT-2 (Baujard et al., 2017).

6.3. Reddish granitic reservoir

At Rittershoffen, the reddish granite is less than 100 m thick in GRT-1 and exhibits the same petrography as in Soultz. The granite is affected by paleo-weathering and hematite deposits. The fracture density is 2.5 fract/m in GRT-1 (Vidal et al., 2016a). The fractures are very scattered but mainly strike N15°E and dip 50°W. An average neutron porosity of 2% was determined from geophysical logs (Vidal et al., 2016c). Open fractures identified on borehole images did not exhibit permeability during drilling operations.

6.4. Sandstones reservoir

The sandstone reservoirs in the Upper Rhine Graben consist of sandstones from Triassic (Buntsandstein) to Permian times. A comparative study of hydraulic data in the URG in Germany and France reveals a mean hydraulic conductivity of 2.4×10^{-7} m/s in Buntsandstein sandstones, compared with 9.6×10^{-7} m/s in granitic basements (Stober and Jodocy, 2009).

At Landau, the Permian formation is thicker than that in Soultz and is called Rotliegendes (Eisbacher and Fielitz, 2010). This sequence consists of coarse clastics (continental conglomerates), fluvial and aeolian sandstones, shales and some evaporites. Triassic sandstones overlie Permian sandstones. Permeable fractures were intersected in the multi-horizon geothermal reservoir (Hettkamp et al., 2007).

At Insheim, the Rotliegendes and Buntsandstein sandstones are approximately 500 m thick and exhibit permeable fractures in both wells (Baumgärtner et al., 2013).

At Rittershoffen, the lithostratigraphy sedimentary cover is similar to that in Soultz (Aichholzer et al., 2015). The neutron porosity is 3% on average in GRT-1 and GRT-2, and is higher when clays are present in the formation (Vidal et al., 2016c). The fracture density is 0.25 fract/m in GRT-1 and 0.4 fract/m in GRT-2 (Vidal et al., 2016a). Fractures in the sandstones are oriented N20°E and dip 70°W in GRT-1, and N170°E with a dip 85°E in GRT-2. Two major clusters with initial permeability intersect GRT-2 and are approximately 20 m and 10 m thick. They are associated with temperature anomalies (Vidal et al., 2017a).

At Cronenbourg, the base of the sedimentary cover in the GCR-1 well consists of Permian sandstones that are overlaid by Triassic sandstones (465 m-thick) (Housse, 1984). The porosity is between 5 and 10%. The main permeable zone is located between 2870 m and 2880 m MD, which coincides with fractured sandstones, whereas sandstones with silica-rich cement are porous but not permeable. The productivity of the sandstone reservoir is estimated to be 0.12 L/s/bar.

At Bruchsal, the exploited geothermal reservoir consists of the Buntsandstein sandstones in GB-1 (> 200 m-thick) and the Buntsandstein and Rotliegendes sandstones in GB-2 (between 150 and

200 m thick for both formations) (Herzberger et al., 2010). Water-bearing fractures control the permeability in the sandstone reservoir (Meixner et al., 2016). The injectivity of the GB-2 well is 0.7 L/s/bar (Kölbel, 2010). The initial productivity of GB-1 is not published.

At Brühl, the targeted geothermal reservoir consists of Buntsandstein sandstones. The fractures are oriented N170°E with an eastward sub-vertical dip (Reinecker et al., 2014). The permeable fault zone intersects between 3150 and 3200 m MD (Melchert et al., 2013). The injectivity index of GT-1 is 3.5 L/s/bar, and the well was not stimulated (Melchert et al., 2013).

6.5. Limestones reservoir

A comparative study of hydraulic data in the URG in Germany and France reveals a mean hydraulic conductivity of 2.0×10^{-6} m/s in Muschelkalk limestones (Stober and Jodocy, 2009).

At Rittershoffen, the Muschelkalk formation is similar to that at Soultz. The fractures are oriented N20°E and dip steeply westward in GRT-1 (Dezayes et al., 2014). These fractures are filled by calcite, quartz and anhydrite. A major permeable fracture zone with drilling mud losses intersects at 1760 m MD in the Middle Muschelkalk in GRT-1 (Baujard et al., 2017).

In the Muschelkalk, permeable zones were also observed in some geothermal wells, including Les Hélicons I, II and III at Preuschoorf, which are less than 10 km westward from Soultz (BRGM, 1993, 1971). The equilibrium temperature reaches 70 °C at approximately 900 m MD. Main inflows of geothermal water are from fractured zones.

At Riehen, in the northeast of Basel, the two wells RB1 and RB2 exploit the aquifer in fractured Muschelkalk limestones (Mégel and Rybach, 2000). The equilibrium temperature reaches 62 °C at 1547 m MD. Fractured zones in Upper Muschelkalk are governed by an advection regime. They control inflows and outflows of geothermal water along the wells.

At Insheim, Muschelkalk is also described as a reservoir, and fracture zones were intersected.

7. Thermal profiles in geothermal wells in the central and southern URG

In the following section, thermal profiles of geothermal wells with equilibrium temperatures > 100 °C at the bottom hole are presented. In Fig. 6, one representative thermal profile was selected for each site and compared to other representative thermal profiles, as well as the respective Soultz reference reservoir.

The well BS-1 at Basel reaches an equilibrium temperature of 174 °C at 4682 m MD (Ladner and Häring, 2009). The thermal profile shows a geothermal gradient of approximately 41 °C/km until 4400 m MD (Fig. 6). In the deepest granitic part, the thermal gradient decreases below 27 °C/km. Low hydraulic yield indicates conductive heat transport.

At Landau, the thermal profile shows a geothermal gradient of 75 °C/km above 2000 m MD (Fig. 6). Below 2000 m MD, the geothermal gradient decreases to approximately 20 °C/km and the equilibrium temperature at the bottom hole reaches 160 °C at 2600 m MD (Schindler et al., 2010). The low geothermal gradient indicates a convection process through permeable fracture zones below 2000 m MD.

At Insheim, equilibrium temperature reaches 160 °C at 3600 m MD, but the thermal profile is not published (Baumgärtner and Lerch, 2013).

At Rittershoffen, the thermal profile shows a high geothermal gradient of 95 °C/km from 0 to 1650 m MD in GRT-1 and from 0 to 1850 m MD (i.e. 0–1650 m True Vertical Depth(TVD)) in GRT-2 (Fig. 6) (Baujard et al., 2017). This uppermost part is associated with conduction processes. The deepest part, from 1650 to 2600 m MD (i.e. 1650–2600 m TVD), exhibits a null geothermal gradient in GRT-1 that indicates a dominant convection process (Baujard et al., 2017). In GRT-2, from 1850 to 3200 m MD (i.e., 1650–2700 m TVD), the geothermal

gradient is low at 18 °C/km. The adiabatic geothermal gradient extends from the hydrothermally altered granite below into to Triassic sediments across the reddish granitic reservoir. All permeable fracture zones intersected by both wells are associated with a positive or negative temperature anomaly (Vidal et al., 2017a). The equilibrium temperature reaches 177 °C at 3196 m MD (Baujard et al., 2017).

At Cronenbourg, the thermal profile shows a high geothermal gradient of 55 °C/km above 2600 m MD (Fig. 6). The Early Muschelkalk limestones, Buntsandstein and Permian sandstones are associated with a convection process and a lower geothermal gradient of 15 °C/km. The temperature at the bottom hole reaches 150 °C at 3200 m MD (Housse, 1984).

At Bruchsal, the thermal profile shows a high geothermal gradient of 50 °C/km above 2300 m MD (Fig. 6). The Buntsandstein and Permian sandstones are associated with null geothermal gradients that indicate a convection process. The equilibrium temperature reaches 135 °C at 2500 m (Herzberger et al., 2010).

At Brühl, the thermal profile shows a geothermal gradient of 45 °C/km (Fig. 6). The convective regime is not clearly evidenced from this thermal profile. The reservoir temperature is approximately 160 °C (Melchert et al., 2013).

8. Relationship among fracture zones and hydrothermal circulations

Convective regimes are associated with geothermal reservoirs in the URG. In the hydrothermally altered granitic reservoirs, geothermal gradients are below 20 °C/km in general. This is interpreted as hydrothermal circulations through the fracture network associated with large-scale normal faults striking N10°W to N20°E. With their relatively important vertical displacement (> 200 m), these faults are interpreted as potential permeable drains for geothermal resources. Hot geothermal fluid upwelling is mainly observed through west-dipping faults (Baillieux et al., 2014). If Permo-Triassic sandstones are also associated with a convective regime at Soultz, Landau, Rittershoffen, Cronenbourg and Bruchsal, then the Muschelkalk limestones mark the top of the convective regime and the switchover towards the conduction regime. This transition between convection and conduction can be smooth, such as that at Soultz and Cronenbourg, or sharp, such as that at Rittershoffen and Bruchsal. Conduction regimes are spatially associated with high geothermal gradients between 50 and 110 °C/km.

The hydraulic yields of the reservoirs are intimately linked to the thermal regimes. Hydrothermal circulations in the deep sedimentary cover and in the hydrothermally altered granitic basement are visible from thermal profiles in geothermal wells in the URG. Moreover, at Soultz as well as at Rittershoffen, permeable fracture zones intersected by wells are associated with thermal anomalies that are either positive or negative. This is interpreted as the thermal signature of the permeable fracture zone.

At Basel, the absence of a clear convection regime suggests that the permeable reservoir was not properly intersected by the well, and hydraulic yields appear to support this assessment (Fig. 6). A thermal profile from the thermal equilibrium of the Brühl well would to decipher the thermal contribution between the conductive and the convective regimes.

The intersection between the wells and the fracture system channelizing the hydrothermal circulations is crucial for geothermal projects; thus, local normal fault zones are the main targets during regional exploration. Because fault zones are steeply dipping, vertical wells have a low probability of intersecting them. The most recent wells drilled in the URG were deviated to intersect the fractured system associated with the fault zone (Landau, Insheim, Rittershoffen, Brühl). These deviated wells show high hydraulic yields that indicate a good connection between open-hole sections and the fractured systems (Fig. 7). The trajectory of the planned geothermal well for the future project at Illkirch (South of Strasbourg) is based on these observations and will be

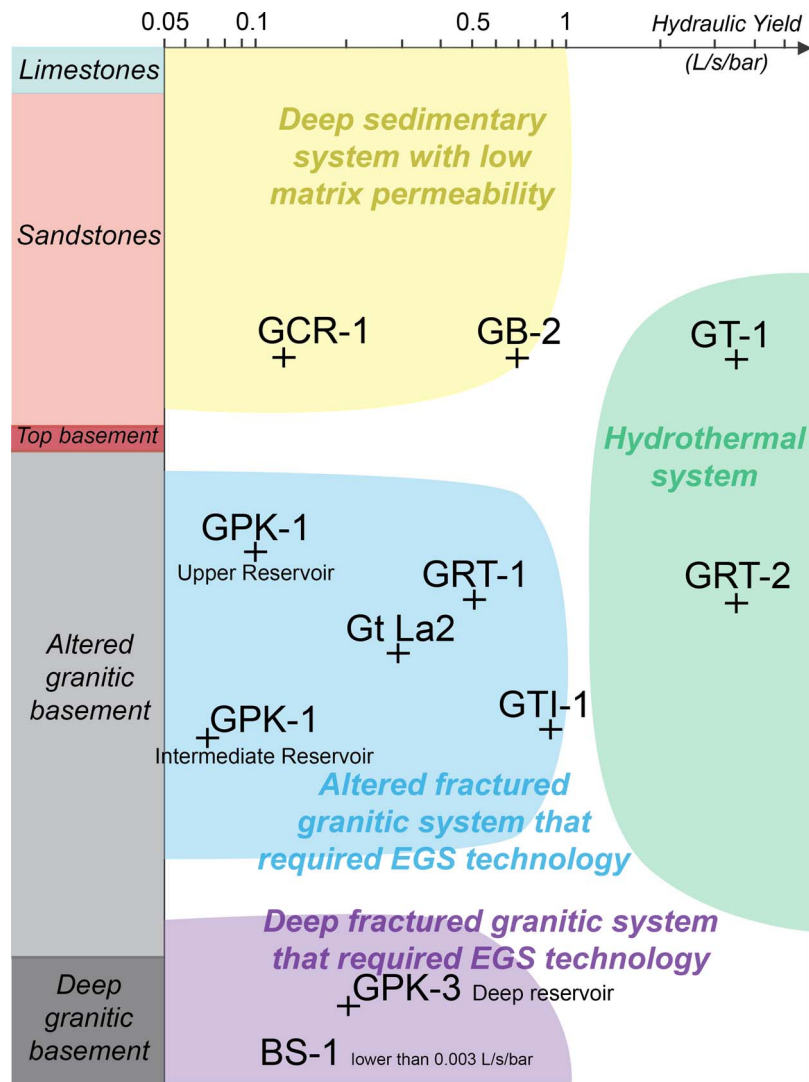


Fig. 7. The hydraulic yield of geothermal wells in the URG is expressed in L/s/bar (Baujard et al., 2017; Baumgärtner et al., 2013; Housse, 1984; Jung and Weidler, 2000; Kölbl, 2010; Ladner and Häring, 2009; Melchert et al., 2013; Schill et al., 2017; Schindler et al., 2010). Hydraulic yields are considered to be before stimulation treatments if there are any. Lithology is from Soultz. Depths for other projects are not at scale. The different varieties of reservoirs are from Ledru and Guillou-Frottier, 2010.

deviated also (Genter et al., 2016).

9. Permeable fracture zones in sedimentary and granitic reservoirs

The architecture of permeable fracture zones is derived from correlations between core samples, cutting observations, acoustic image logs and standard geophysical logs (caliper, gamma ray, neutron porosity...) (Fig. 5) (Dezayes et al., 2010b; Genter et al., 1992; Genter and Traineau, 1992; Traineau et al., 1992). The permeability at the borehole scale is estimated from anomalies on temperature logs, flow logs, mud losses and gas occurrences (Bradford et al., 2013; Davatzes and Hickman, 2005; Dezayes et al., 2010b; Genter et al., 2010; Mas et al., 2006).

Permeable fractures were intersected in deep granite in the deepest sections of the Soultz and Basel wells. At Soultz, a fault plane intersected through GPK-3 (Sausse et al., 2010). The fault zone is approximately 25 m thick. The fault core is composed mainly of permeable drains that are approximately 10 cm to 20 cm thick. The damage zone consists of 7 individual fractures. At Basel, the fracture zones are very localized and poorly connected.

Permeable fracture zones were intersected through hydrothermally altered granite at Soultz, Rittershoffen, and likely Insheim and Landau

as well. At Soultz, these zones are approximately 25–40 m thick. They consist of a fault core with a high fracture density and main permeable drains that are 10 cm thick (Genter et al., 2000). Main permeable drains are partly sealed with geodic quartz (Fig. 8). The surrounded damage zone is highly altered and porous and is composed of more than 100 tiny fractures that are likely connected at the borehole scale (Fig. 8). Despite the high porosity values in the damage zone, well tests reveal that 95% of the flow entered the rock mass at only 10 discrete flow points, which correspond to main opened fractures observed on acoustic image logs (Evans et al., 2005). At Rittershoffen, a branch of the Rittershoffen fault likely intersected through GRT-1 and GRT-2 (Baujard et al., 2017). At the borehole scale, this fault zone is 40 m thick. In GRT-1, the main permeable drain is 25 cm thick and is topped by a damage zone that consists of 50 fractures in GRT-1 (Fig. 8). In GRT-2, several thick permeable drains are surrounded by many tiny fractures. At Insheim, permeable fracture zones are 10–15 m thick.

The top of the granitic basement is an altered and fractured formation that acts as a tight reservoir because of secondary mineral precipitation and especially clay minerals and is therefore not considered to be permeable (Vidal et al., 2017b, 2016c).

Permeable fracture clusters were intersected through sandstones at Bruchsal, Cronenbourg, Rittershoffen and likely Insheim. These clusters exhibit a thickness between 10 and 20 m with no obvious displacement

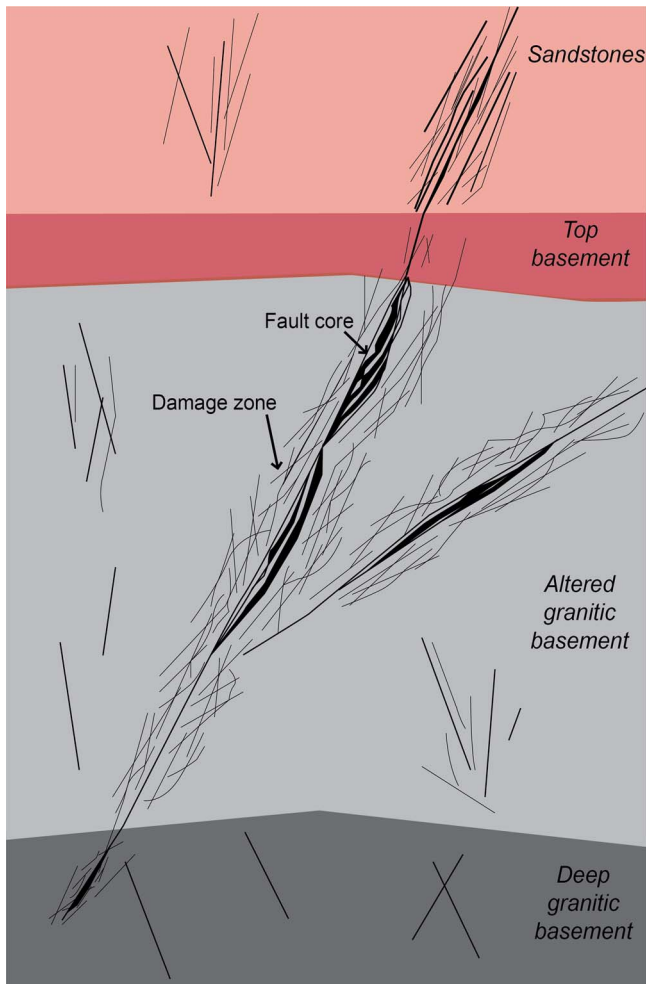


Fig. 8. Fault zone architecture in sandstone, hydrothermally altered granite and deep granite. FZ = Fault Zone, FC = Fault Core, DZ = Damage Zone.

observed. At Soultz, a branch of the Soultz fault intersects EPS-1 and GPK-1 in the Vosgian sandstones (Sausse et al., 2010). The fault zone is approximately 50 m thick. The fault core consists of main permeable drains that are 5 cm thick (Vernoux et al., 1995). The damage zone consists of more than 50 individual fractures. At Brühl, a local fault zone was also intersected through sandstones that are up to 100 m thick (Melchert et al., 2013; Reinecker et al., 2014).

Deep sedimentary reservoirs and deep granitic reservoirs show lower permeability than altered granitic reservoirs (Fig. 5). This difference in permeability could be explained by a structural difference in the architecture of fault zones in sediments, hydrothermally altered granite and deep granite. A high density of macro-scale fractures favors intersection, and thus connectivity. This highly clustered organization could sustain permeability. The fault zones in the hydrothermally altered granite consist of a thick fault core that is characterized by a high fracture density and a porous, altered and fractured damage zone (Fig. 8). This large damage zone could extend several dozen meters around the fault core; thus, several fault zones are well-connected to the large-scale fracture network. The permeability of fault zones is a first-order permeability that responds locally and rapidly (Sausse and Genter, 2005). However thick permeable fractures are connected to a wide and regular network of small-scale fractures affecting the whole granitic batholith and responding to a larger scale of permeability. The fault zones in the deep granite are more localized. Even if the fault cores are thick, the fracture density in the damage zone is less important, so the connectivity in the fracture network is poorer. The fault zones in deep sediments exhibit thinner fault cores than those in granite and

large damage zones, where fracture clusters promote permeability. These zones are less prevalent in sediments than in granite.

10. Concluding remarks

The Soultz-sous-Forêts project was an important scientific contribution for the deep geothermal development in the Upper Rhine Graben. The permeability is supported by the major fracture network. Drilling more than 20 km at Soultz in the sedimentary cover and in the granitic basement reveals geothermal brine circulating into the natural fracture network. This convection system leads to the thermal anomaly. The experience at Soultz makes the HDR technology, which aims to create a deep geothermal reservoir in low-permeability crystalline rocks, obsolete. It demonstrates the feasibility of the EGS technology in the URG and aims to reactivate and connect preexisting fractures into a large-scale fractured reservoir by thermal, chemical and hydraulic treatments. The experience at Soultz reveals that the first 500 m of the granitic basement, highly fractured and hydrothermally altered, is a higher potential reservoir. Fault zones present a higher permeability for hydrothermally altered granitic basements than for hard fractured sandstones or poorly altered deep granitic basements, likely due to their intense fracture density in the fault core and their larger damage zone, which allow connection with the reservoir. The larger roughness of the fracture surface in the granite is also key for explaining the self-propping of fractures after the stimulation. The Soultz sedimentary reservoir and the deep sedimentary wells (GCR-1, Les Héliens, GT-1) demonstrated that permeability is supported by fracture zones and not by a porous matrix. The porosity associated with fractures in the sediments is lower than in the hydrothermally altered granitic basements.

Following industrial projects (Landau, Insheim, Rittershoffen, Brühl) were based on the lessons learned at Soultz. For most of these projects the permeability of fracture zones is higher in the hydrothermally altered granitic reservoir. The permeability is intimately linked to the sub-vertical fault zone in the URG that strikes N-S and dips westward. Wells target local fault zones at the sediments-basement interface. Depths of geothermal wells were divided by two compared to Soultz, and the flowrate was increased more than two fold. Development of reservoir in the top of the hydrothermally altered granitic basement is economically more interesting. Inclined trajectories allow for a higher connection between the well and the sub-vertical fault zone, and thus a higher natural permeability. If the well trajectory is correctly designed according to the fault zone's geometry, geothermal wells exhibit sufficient hydrothermal permeability for industrial exploitation and do not need to be stimulated as observed at Rittershoffen (GRT-2), Brühl (GT-1) or Insheim (GTI-2). These recent geothermal wells qualify as hydrothermal wells. The absence of stimulation is a substantial advantage in terms of environmental effects and for the public acceptance of future geothermal projects. However, the localization of faults at the top of the granitic basement at the seismic scale is less uncertain. Two-dimensional seismic profiles imaged the sedimentary cover but poorly imaged the top of the basement (Sausse et al., 2010). Major faults at the seismic scale that cross-cut the sedimentary cover in seismic interpretations are extended downwards into the deep basement. Future geothermal projects will require technical innovation of exploration methods to accurately characterize the fractured system at the top of the basement. Experience with 3D seismic profiles for the geothermal project in Brühl showed promising results to accurately identify the geometry of faults at the sediment-basement interface (Lotz, 2013).

Acknowledgments

This work was performed in the framework of the LabEx G-Eau-Thermie Profonde which was co-funded by the French government under the program "Investissements d'Avenir", and as a contribution to the PhD thesis of Jeanne Vidal, who was co-funded by ADEME (French

Agency for Environment and Energy). A portion of this work was conducted in the framework of the EGS Alsace project, which was cofunded by ADEME and ES. The authors are grateful to GEIE EMC (Soulz) and ECOGI (Rittershoffen) for accessing to geological and geophysical data. Dr Chrystel Dezayes from BRGM and Dr Clément Baujard from ES-Géothermie are also acknowledged for their support. The authors appreciate the helpful and constructive remarks of an anonymous reviewer, Dr Harald Milsch and the editor-in-Chief Dr Eva Schill which seriously improved the manuscript.

References

- Aichholzer, C., Düringer, P., Orciani, S., Genter, A., 2015. New stratigraphic interpretation of the twenty-eight-year old GPK-1 geothermal well of Soultz-sous-Forêts (Upper Rhine Graben, France). In: Proceedings of the 4th European Geothermal Workshop. Strasbourg, France.
- Altherr, R., Henes-Klaiber, U., Hegner, E., Satir, M., Langer, C., 1999. Plutonism in the Variscan Odenwald (Germany): from subduction to collision. *Int. J. Earth Sci.* 88, 422–443. <http://dx.doi.org/10.1007/s005310050276>.
- Altherr, R., Holl, A., Hegner, E., Langer, C., Kreuzer, H., 2000. High-potassium, calc-alkaline I-type plutonism in the European variscides: northern vosges (France) and northern schwarzwald (Germany). *Lithos* 50, 51–73. [http://dx.doi.org/10.1016/S0024-4937\(99\)00052-3](http://dx.doi.org/10.1016/S0024-4937(99)00052-3).
- Aquilina, L., Pauwels, H., Genter, A., Fouillac, C., 1997. Water-rock interaction processes in the Triassic sandstone and the granitic basement of the Rhine Graben: geochemical investigation of a geothermal reservoir. *Geochim. Cosmochim. Acta* 61, 4281–4295. [http://dx.doi.org/10.1016/S0016-7037\(97\)00243-3](http://dx.doi.org/10.1016/S0016-7037(97)00243-3).
- Aquilina, L., Brach, M., Foucher, J.C., De Las Heras, A., Braibant, G., 1993. Deepening of GPK-1 HDR Borehole 2000–3600 m (Soulz-sous-Forêts, France), Geochemical Monitoring of Drilling Fluids (Open File No. R36619). BRGM, Orléans, France.
- Bächler, D., Kohl, T., Rybach, L., 2003. Impact of graben-parallel faults on hydrothermal convection-Rhine Graben case study. *Phys. Chem. Earth* 28, 341–441. [http://dx.doi.org/10.1016/s1474-7065\(03\)00063-9](http://dx.doi.org/10.1016/s1474-7065(03)00063-9).
- BRGM, 1971. Forage d'eau Thermominérale 1266 – Rapport SGAL (Open File No. 71-SGN-244-SGA). BRGM, Orléans, France.
- BRGM, 1993. Recherche de nouvelles ressources en eaux thermales à Merckwiller-Pechelbronn (67). *Compte rendu des travaux de réalisation du forage HELION III* (Open file No. N-0549-STR-4S-93). BRGM, Orléans, France.
- Baillieux, P., Schill, E., Edel, J.-B., Mauri, G., 2013. Localization of temperature anomalies in the Upper Rhine Graben: insights from geophysics and neotectonic activity. *Int. Geol. Rev.* 55, 1744–1762. <http://dx.doi.org/10.1080/00206814.2013.794914>.
- Baillieux, P., Schill, E., Abdelfettah, Y., Dezayes, C., 2014. Possible natural fluid pathways from gravity pseudo-tomography in the geothermal fields of Northern Alsace (Upper Rhine Graben). *Geotherm. Energy* 2. <http://dx.doi.org/10.1186/s40517-014-0016-y>.
- Baria, R., Garnish, J., Baumgärtner, J., Gérard, A., Jung, R., 1995. Recent developments in the European HDR research programme at Soultz-sous-Forêts (France). In: Proceedings of World Geothermal Congress 1995. Florence, Italy.
- Bartier, D., Ledéret, B., Clauer, N., Meunier, A., Liewig, N., Morvan, G., Addad, A., 2008. Hydrothermal alteration of the Soultz-sous-Forêts granite (Hot Fractured Rock geothermal exchanger) into a tosubite and illite assemblage. *Eur. J. Miner.* 20, 131–142. <http://dx.doi.org/10.1127/0935-1221/2008/0020-1787>.
- Baujard, C., Genter, A., Dalmais, E., Maurer, V., Hehn, R., Rosillette, R., Vidal, J., Schmittbuhl, J., 2017. Hydrothermal characterization of wells GRT-1 and GRT-2 in Rittershoffen, France: implications on the understanding of natural flow systems in the rhine graben. *Geothermics* 65, 255–268. <http://dx.doi.org/10.1016/j.geothermics.2016.11.001>.
- Baumgärtner, J., Lerch, C., 2013. Geothermal 2.0: the insheim geothermal power plant: the second generation of geothermal power plants in the upper rhine graben. In: Proceedings of Third European Geothermal Review. Mainz, Germany.
- Baumgärtner, J., Gérard, A., Baria, R., 2000. Soultz-sous-Forêts: main technical aspects of deepening the well GPK2. In: Proceedings of World Geothermal Congress 2000. Kyushu – Tohoku, Japan.
- Baumgärtner, J., Teza, D., Wahl, G., 2013. Gewinnung geothermischer Energie durch Entwicklung und Zirkulation eines Störungssystems im Kristallin und deren mikro-seismische Überwachung am Beispiel des Geothermieprojektes Insheim (Internal Report No. 0325158). (Bestec GmbH, Landau, Germany).
- Baumgärtner, J., 2007. The geox GmbH project in Landau – The first geothermal power project in Palatinate/Upper Rhine Valley. In: Proceedings of First European Geothermal Review. Mainz, Germany.
- Benderitter, Y., Tabbagh, A., Elsass, P., 1995. Calcul de l'effet thermique d'une remontée hydrothermale dans le socle fracturé. Application à l'anomalie géothermique de Soultz-sous-Forêts (Nord Alsace). *Bulletin de la Société Géologique de France* 1, 37–48.
- Bergerat, F., 1985. Déformations cassantes et champs de contrainte tertiaires dans la plate-forme européenne (Habilitation à Diriger la Recherche). Université Pierre et Marie Curie-Paris VI, France.
- Bradford, J., McLennan, J., Moore, J., Glasby, D., Waters, D., Kruwells, R., Bailey, A., Rickard, W., Bloomfield, K., King, D., 2013. Recent developments at the Raft River geothermal field. In: Proceedings of Thirty-Eighth Workshop on Geothermal Reservoir Engineering. Stanford University, California, USA.
- Cautru, J.-P., 1988. Coupe géologique passant par le forage GPK-1 calée sur la sismique réflexion (Technical report). BRGM, Institut Mixte de Recherches Géothermiques, France.
- Cocherie, A., Guerrot, C., Fanning, M.C., Genter, A., 2004. Datation U-Pb des deux faciès du granite de Soultz (Fossé Rhénan, France). *C.R. Geosci.* 336, 775–787. <http://dx.doi.org/10.1016/j.crte.2004.01.009>.
- Cuenot, N., Dorbath, L., 2008. Analysis of the microseismicity induced by fluid injections at the EGS site of Soultz-sous-Forêts (Alsace, France): Implications for the characterization of the geothermal reservoir properties. *Pure Appl. Geophys.* 165, 797–828. <http://dx.doi.org/10.1007/s00024-008-0335-7>.
- Davatzes, N.C., Hickman, S.H., 2005. Controls on fault-hosted fluid flow; Preliminary results from the Coso Geothermal Field, CA. *Geothermal Resources Council Transactions Geothermal Resources Council* 29, pp. 343–348.
- Dèzes, P., Schmid, S.M., Ziegler, P.A., 2004. Evolution of the European Cenozoic Rift System: interaction of the Alpine and Pyrenean orogens with their foreland lithosphere. *Tectonophysics* 389, 1–33. <http://dx.doi.org/10.1016/j.tecto.2004.06.011>.
- Degouy, M., Villeneuve, B., Weber, R., 1992. Logistical Support and Development of the Soultz Hot Dry Rock Site: Seismic Observation Wells and Well EPS-1, Final Drilling Report (No. RR-41179-FR). BRGM, Commission of European Communities, Bruxelles, Belgique.
- Dezayes, C., Genter, A., Homeier, G., Degouy, M., Stein, G., 2003. Geological Study of GPK-3 HFR Borehole (Soulz-sous-Forêts, France) (Open File Report No. RP-52311-FR). BRGM, Orléans, France.
- Dezayes, C., Chèvremont, P., Tourlière, B., Homeier, G., Genter, A., 2005a. Geological Study of the GPK4 HFR Borehole and Correlation with the GPK3 Borehole (Soulz-sous-Forêts, France) (Open File Report No. RP-53697-FR). BRGM, Orléans, France.
- Dezayes, C., Genter, A., Genter, S., 2005b. Deep Geothermal Energy in Western Europe: the Soultz Project – Final Report (Open File No. BRGM/RP-54227-FR). BRGM, Orléans, France.
- Dezayes, C., Courrioux, G., Calcagno, P., Tourlière, B., Chèvremont, P., Sausse, J., Place, J., 2010a. Des données géologiques aux modèles 3D du site EGS de Soultz-sous-Forêts (Alsace, France) (Final report, Open file No. BRGM/RP-57927-FR). BRGM, Orléans, France.
- Dezayes, C., Genter, A., Valley, B., 2010b. Structure of the low permeable naturally fractured geothermal reservoir at Soultz. *C.R. Geosci.* 342, 517–530. <http://dx.doi.org/10.1016/j.crte.2009.10.002>.
- Dezayes, C., Sanjuan, B., Gal, F., Lerouge, C., 2014. Fluid geochemistry monitoring and fractured zones characterization in the GRT1 borehole (ECOGI project, Rittershoffen, Alsace, France). In: Proceedings of Deep Geothermal Days. Paris, France.
- Dezayes, C., Lerouge, C., Sanjuan, B., Ramboz, C., Brach, M., 2015. Toward a better understanding of the fluid circulation in the Rhine Graben for a better geothermal exploration of the deep basins. In: Proceedings of World Geothermal Congress 2015. Melbourne, Australia.
- Doebf, F., 1967. The tertiary and pleistocene sediments of the Northern and Central part of the upper Rhinegraben. *Mémoires du Service de la carte géologique d'Alsace et de Lorraine*. pp. 48–54.
- Dubois, M., Ledéret, B., Potdevin, J.-L., Vançon, S., 2000. Détermination des conditions de précipitation des carbonates dans une zone d'altération du granite de Soultz (soubassement du fossé Rhénan, France): l'enregistrement des inclusions fluides. *Comptes Rendus de l'Académie des Sciences – Series IIA – Earth and Planetary Science* 331, pp. 303–309. [http://dx.doi.org/10.1016/S1251-8050\(00\)01429-4](http://dx.doi.org/10.1016/S1251-8050(00)01429-4).
- Edel, J.-B., Schulmann, K., 2009. Geophysical constraints and model of the Saxothuringian and Rhenohercynian subductions – magmatic arc system in NE France and SW Germany. *Bull. Soc. Geol. Fr.* 180, 545–558. <http://dx.doi.org/10.2113/gssgfbull.180.6.545>.
- Edel, J.B., Weber, K., 1995. Cadomian terranes, wrench faulting and thrusting in the central Europe Variscides: geophysical and geological evidence. *Geol. Rundsch.* 84, 412–432. <http://dx.doi.org/10.1007/BF00260450>.
- Edel, J.-B., Schulmann, K., Rotstein, Y., 2007. The Variscan tectonic inheritance of the Upper Rhine Graben: evidence of reactivations in the Lias, Late Eocene–Oligocene up to the recent. *Int. J. Earth Sci.* 96, 305–325. <http://dx.doi.org/10.1007/s00531-006-0092-8>.
- Eisbacher, G.H., Fielitz, W., 2010. Karlsruhe und seine Region. Nordschwarzwald, Kraichgau, Neckartal, südlicher Odenwald, Oberrhein-Graben, Pfälzerwald und westliche Schwäbische Alb. *Borntraeger Science Publishers, Stuttgart, Germany*.
- Evans, K., Genter, A., Sausse, J., 2005. Permeability creation and damage due to massive fluid injections into granite at 3.5 km at Soultz : 1. Borehole observations. *J. Geophys. Res.* 110. <http://dx.doi.org/10.1029/2004JB003168>.
- Fuchs, K., Bonjer, K., Gajewski, D., Lüschen, E., Prodehl, C., Sandmeier, K., Wenzel, F., Wilhelm, H., 1987. Crustal evolution of the Rhinegraben area. 1. Exploring the lower crust in the Rhinegraben rift by unified geophysical experiments. *Tectonophysics* 141, 261–275.
- Gérard, A., Kappelmeier, O., 1987. Le projet géothermique européen de Soultz-sous-Forêts: situation au 1er janvier 1988. *Geothermics* 16, 393–399. [http://dx.doi.org/10.1016/0375-6505\(87\)90018-6](http://dx.doi.org/10.1016/0375-6505(87)90018-6).
- Géraud, Y., Rosener, M., Surma, F., Place, J., Le Garzic, É., Diraison, M., 2010. Physical properties of fault zones within a granite body: example of the Soultz-sous-Forêts geothermal site. *C.R. Geosci.* 342, 566–574. <http://dx.doi.org/10.1016/j.crte.2010.02.002>.
- GeORG Team, 2013. Potentiel géologique profond du Fossé rhénan supérieur. Rapport final du projet GeORG –INTERREG IV –Partie 2: géologie et potentiel (Open File Report).
- GeORG, 2012. Geoportail of EU-Project GeORG – INTERREG IV Upper Rhine. [WWW Document], URL <http://www.geopotenziale.org> (Accessed 14 April 2016).
- Genter, A., Tenzer, H., 1995. Geological Monitoring of GPK-2 HDR Borehole, 1420–3880 m (Soulz-sous-Forêts) (Open File Report No. R38629). BRGM, Orléans, France.
- Genter, A., Traineau, H., 1992. Borehole EPS1, Alsace, France: preliminary geological

- results from granite core analyses for Hot Dry Rock research. *Sci. Drill.* 3, 205–214.
- Genter, A., Traineau, H., 1996. Analysis of macroscopic fractures in granite in the HDR geothermal well EPS-1, Soultz-sous-Forêts, France. *J. Volcanol. Geotherm. Res.* 72, 121–141. [http://dx.doi.org/10.1016/0377-0273\(95\)00070-4](http://dx.doi.org/10.1016/0377-0273(95)00070-4).
- Genter, A., Martin, P., Montaggioni, P., 1992. Application of FMS and BHTV tools for evaluation of natural fractures in the Soultz geothermal borehole GPK-1. In: Bresee, James C. (Ed.), *Geothermal Energy in Europe – The Soultz Hot Dry Rock Project*. Gordon and Breach Science Publishers, Montreux, Switzerland, pp. 69–82.
- Genter, A., Castaing, C., Dezayes, C., Tenzer, H., Traineau, H., Villemain, T., 1997a. Comparative analysis of direct (core) and indirect (borehole imaging tools) collection of fracture data in the Hot Dry Rock Soultz reservoir (France). *J. Geophys. Res.* 102 (15), 415–419. <http://dx.doi.org/10.1029/97JB00626>.
- Genter, A., Traineau, H., Artignan, D., 1997b. Synthesis of geological and geophysical data at Soultz-sous-Forêts (France) (Open file report No. BRGM/R 39440). BRGM.
- Genter, A., Traineau, H., Ledéret, B., Bourguine, B., Gentier, S., 2000. Over 10 years of geological investigations within the HDR Soultz project, France. In: *Proceedings of World Geothermal Congress 2000*. Kyushu – Tohoku, Japan.
- Genter, A., Evans, K., Cuenot, N., Fritsch, D., Sanjuan, B., 2010. Contribution of the exploration of deep crystalline fractured reservoir of Soultz to the knowledge of enhanced geothermal systems (EGS). *C.R. Geosci.* 342, 502–516. <http://dx.doi.org/10.1016/j.crte.2010.01.006>.
- Genter, A., Baujard, C., Cuenot, N., Dezayes, C., Kohl, T., Masson, F., Sanjuan, B., Scheiber, J., Schill, E., Schmittbuhl, E., Vidal, J., 2016. Geology, Geophysics and Geochemistry in the Upper Rhine Graben: the frame for geothermal energy use. In: *Proceedings of European Geothermal Congress 2016*. Strasbourg, France.
- Grecksch, G., Ortiz, A., Schellschmidt, R., 2003. Thermophysical Study of GPK2 and GPK3 Granite Samples: HDR Project Soultz Report. GGA-Bericht, Hannover, Germany.
- Griffiths, L., Heap, M.J., Wang, F., Daval, D., Gilg, H.A., Baud, P., Schmittbuhl, J., Genter, A., 2016. Geothermal implications for fracture-filling hydrothermal precipitation. *Geothermics* 64, 235–245. <http://dx.doi.org/10.1016/j.geothermics.2016.06.006>.
- Häring, M.O., Schanz, U., Ladner, P., Dyer, B.C., 2008. Characterisation of the Basel 1 enhanced geothermal system. *Geothermics* 37, 469–495. <http://dx.doi.org/10.1016/j.geothermics.2008.06.002>.
- Haffen, S., Géraud, Y., Diraison, M., Dezayes, C., 2013. Determining fluid-flow zones in a geothermal sandstone reservoir from thermal conductivity and temperature logs. *Geothermics* 46, 32–41. <http://dx.doi.org/10.1016/j.geothermics.2012.11.001>.
- Hehn, R., Genter, A., Vidal, J., Baujard, C., 2016. Stress field rotation in the EGS well GRT-1 (Rittershoffen, France). In: *Proceedings of European Geothermal Congress 2016*. Strasbourg, France.
- Herbrich, B., 1988. Le forage géothermique de Soultz-sous-Forêts (GPK1), Rapport de fin de sondage (No. 29421). CFG, Orléans, France.
- Herzberger, P., Münch, W., Kölbl, T., Bruchmann, U., Schlagermann, P., Hölzt, H., Wolf, L., Rettenmaier, D., Steger, H., Zorn, R., Seibt, P., Möllmann, G.-U., Ghergut, J., Ptak, T., 2010. The geothermal power plant Bruchsal. In: *Proceedings of World Geothermal Congress 2010*. Bali, Indonesia.
- Hettkamp, T., Baumgärtner, J., Baria, R., Gérard, A., Gandy, T., Michelet, S., Teza, D., 2004. Electricity production from hot rocks. In: *Proceedings of Twenty-Ninth Workshop on Geothermal Reservoir Engineering*. University of Stanford, California, USA.
- Hettkamp, T., Teza, D., Baumgärtner, J., Gandy, T., Homeier, G., 2007. A multi-horizon approach for the exploration and exploitation of a fractured geothermal reservoir in Landau/Palatine. In: *Proceedings of First European Geothermal Review*. Mainz, Germany.
- Housse, B.A., 1984. Reconnaissance du potentiel géothermique du Buntsandstein à Strasbourg—Cronenburg. *Géotherm. Actual.* 1.
- Illies, H.J., Greiner, G., 1979. Holocene movements and state of stress in the rhinegraben rift system. *Tectonophysics. Recent Crustal Mov.* 52, 349–359. [http://dx.doi.org/10.1016/0040-1951\(79\)90245-2](http://dx.doi.org/10.1016/0040-1951(79)90245-2).
- Illies, H.J., 1965. Bauplan und baugeschichte des oberrheingrabens. *Oberrheinische Geol. Abh.* 14, 1–54.
- Illies, H.J., 1972. The Rhine graben rift system-plate tectonics and transform faulting. *Geophys. Surv.* 1, 27–60. <http://dx.doi.org/10.1007/bf01449550>.
- Jung, R., Weidler, R., 2000. A conceptual model for the stimulation process of the HDR-system at Soultz. *Geothermal Resources Council Transactions* 24, pp. 143–147.
- Jung, R., 1992. Hydraulic fracturing and hydraulic testing in the granitic section of borehole GPK-1, Soultz-sous-Forêts. In: Bresee, James C. (Ed.), *Geothermal Energy in Europe – The Soultz Hot Dry Rock Project*. Gordon and Breach Science Publishers, Montreux, Switzerland, pp. 149–198.
- Käser, B., Kalt, A., Borel, J., 2007. The crystalline basement drilled at the Basel-1 geothermal site. A preliminary petrological-geochemical study. In: *Report to Geopower Basel AG for Swiss Deep Heat Mining Project Basel*. Institut de Géologie et d'Hydrogéologie, Université de Neuchâtel, Switzerland.
- Kölbl, T., 2010. Geothermal power plant Bruchsal: construction and initial operating experiences. In: *Proceedings of Third European Geothermal Review*. Mainz, Germany.
- Ladner, F., Häring, M.O., 2009. Hydraulic characteristics of the Basel 1 Enhanced Gbase1 1 enhanced geothermal system. *Geothermal Resources Council Transactions* 33, pp. 199–204.
- Lagarde, J.L., Capdevila, R., Fourcade, S., 1992. Granites et collision continentale; l'exemple des granitoïdes carbonifères dans la chaîne hercynienne ouest-européenne. *Bull. Soc. Geol. Fr.* 163, 597–610.
- Ledéret, B., Berger, G., Meunier, A., Genter, A., Bouchet, A., 1999. Diagenetic-type reactions related to hydrothermal alteration in the Soultz-sous-Forêts Granite, France. *Eur. J. Mineral.* 11, 731–741. <http://dx.doi.org/10.1127/ejm/11/4/0731>.
- Ledru, P., Guillou-Frotier, L., 2010. Reservoir definition. In: *Geothermal Energy Systems – Exploration, Development, and Utilization* Ernst Huenges. Weinheim, Germany. pp. 1–36.
- Lorenz, V., Nicholls, I.A., 1976. The Permian Carboniferous Basin and Range province of Europe. An application of plate tectonics. In: Falke, H. (Ed.), *The Continental Permian in Central, West, and South Europe: Proceedings of the NATO Advanced Study Institute*. Dordrecht, Holland. pp. 313–342. http://dx.doi.org/10.1007/978-94-010-1461-8_22.
- Lotz, U., 2013. Specific challenges for geothermal projects in Baden-Württemberg – geothermal project Brühl. In: *Proceedings of Third European Geothermal Review*. Mainz, Germany.
- Mégel, T., Rybach, L., 2000. Production capacity and sustainability of geothermal doublets. In: *Proceedings of World Geothermal Congress 2000*. Kyushu – Tohoku, Japan.
- Mas, A., Guisseau, D., Patrier, P., Beaufort, D., Genter, A., Sanjuan, B., Girard, J.P., 2006. Clay minerals related to the hydrothermal activity of the Bouillante geothermal field (Guadeloupe). *J. Volcanol. Geotherm. Res.* 158, 380–400. <http://dx.doi.org/10.1016/j.jvolgeores.2006.07.010>.
- Meixner, J., Schill, E., Gaucher, E., Kohl, T., 2014. Inferring the in situ stress regime in deep sediments: an example from the Bruchsal geothermal site. *Geotherm. Energy* 2. <http://dx.doi.org/10.1186/s40517-014-0007-z>.
- Meixner, J., Schill, E., Grimmer, J.C., Gaucher, E., Kohl, T., Klingler, P., 2016. Structural control of geothermal reservoirs in extensional tectonic settings: an example from the Upper Rhine Graben. *J. Struct. Geol.* 82, 1–15. <http://dx.doi.org/10.1016/j.jsg.2015.11.003>.
- Melchert, B., Stober, I., Lotz, U., 2013. Erste ergebnisse der hydraulischen testmaßnahmen und geochemischen analysen der geothermie-bohrung GT1 in Brühl/Baden-Württemberg. In: *Presented at the Geothermiekongress 2013*. Essen, Germany.
- Meller, C., Kohl, T., 2014. The significance of hydrothermal alteration zones for the mechanical behavior of a geothermal reservoir. *Geotherm. Energy* 2, 1–21. <http://dx.doi.org/10.1186/s40517-014-0012-2>.
- Nami, P., Schellschmidt, R., Schindler, M., Tischner, T., 2008. Chemical stimulation operations for reservoir development of the deep crystalline HDR/EGS system at Soultz-sous-Forêts (France). In: *Proceedings of Thirty-Second Workshop on Geothermal Reservoir Engineering*. Stanford University, California, USA.
- Pauwels, H., Fouillac, C., Fouillac, A.-M., 1993. Chemistry and isotopes of deep geothermal saline fluids in the Upper Rhine Graben: origin of compounds and water-rock interactions. *Geochim. Cosmochim. Acta* 57, 2737–2749. [http://dx.doi.org/10.1016/0016-7037\(93\)90387-C](http://dx.doi.org/10.1016/0016-7037(93)90387-C).
- Portier, S., Vuataz, F.-D., Nami, P., Sanjuan, B., Gérard, A., 2009. Chemical stimulation techniques for geothermal wells: experiments on the three-well EGS system at Soultz-sous-Forêts, France. *Geothermics* 38, 349–359. <http://dx.doi.org/10.1016/j.geothermics.2009.07.001>.
- Pribnow, D., Clauser, C., 2000. Heat and fluid flow at the Soultz Hot Dry Rock system in the Rhine Graben. In: *Proceedings of World Geothermal Congress 2000*. Kyushu – Tohoku, Japan.
- Pribnow, D., Schellschmidt, R., 2000. Thermal tracking of upper crustal fluid flow in the Rhine Graben. *Geophys. Res. Lett.* 27.
- Pribnow, D., 2000. The Deep Thermal Regime in Soultz and Implications for Fluid Flow: HDR Project Soultz Report. GGA-Bericht, Hannover.
- Lummer, N., Rauf, O., Gerdes, S., Genter, A., Scheiber, J., Villadangos, G., 2014. New biodegradable stimulation system – First field trial in granite/Bunter sandstone formation for a geothermal application in the Upper Rhine Valley. In: *Proceedings of Deep Geothermal Days*. Paris, France.
- Reinecker, J., Bauer, J., Philipp, S.L., 2014. Fault zones and associated fracture systems in geothermal exploration. In: *Presented at the Tiefengeothermie – Forum*. Hessen, Germany.
- Ritter, J., Fritsch, M., Gassner, L., Groos, J., Grund, M., Zeiss, J., 2014. Mechanism of fluid-induced micro-earthquakes near Landau, Upper Rhine Graben, Germany. In: *Proceedings of European Geosciences Union 2014*. Wien, Austria.
- Rueter, H., 2010. Oral Communication at Workshop on Induced Seismicity Due to Fluid Injection/production from Energy-related Applications. Stanford University, California USA.
- Rummel, F., Haack, U., Gohn, E., 1988. Uranium, Thorium and Potassium Content and Derived Heat Production Rate (Yellow Report No. 6–9). Ruhr Universität, Bochum, Germany.
- Rummel, F., 1992. Physical properties of the rock in the granite section of borehole GPK-1, Soultz-sous-Forêts. In: Bresee, James C. (Ed.), *Geothermal Energy in Europe – The Soultz Hot Dry Rock Project*. Gordon and Breach Science Publishers, Montreux, Switzerland, pp. 199–216.
- Sanjuan, B., Millot, R., Dezayes, C., Brach, M., 2010. Main characteristics of the deep geothermal brine (5 km) at Soultz-sous-Forêts (France) determined using geochemical and tracer test data. *CR Geosci.* 342, 546–559. <http://dx.doi.org/10.1016/j.crte.2009.10.009>.
- Sanjuan, B., Millot, R., Ásmundsson, R., Brach, M., Giroud, N., 2014. Use of two new Na/Li geothermometric relationships for geothermal fluids in volcanic environments. *Chem. Geol.* 389, 60–81. <http://dx.doi.org/10.1016/j.chemgeo.2014.09.011>.
- Sanjuan, B., Millot, R., Innocent, C., Dezayes, C., Scheiber, J., Brach, M., 2016. Major geochemical characteristics of geothermal brines from the Upper Rhine Graben granitic basement with constraints on temperature and circulation. *Chem. Geol.* 428, 27–47. <http://dx.doi.org/10.1016/j.chemgeo.2016.02.021>.
- Sausse, J., Genter, A., 2005. Types of permeable fractures in granite. *Geol. Soc. London* 240, 1–14. <http://dx.doi.org/10.1144/GSL.SP.2005.240.01.01>. Special Publications.
- Sausse, J., Dezayes, C., Dorbath, L., Genter, A., Place, J., 2010. 3D model of fracture zones at Soultz-sous-Forêts based on geological data, image logs, induced microseismicity and vertical seismic profiles. *C.R. Geosci.* 342, 531–545. <http://dx.doi.org/10.1016/j.crte.2010.01.011>.
- Schad, A., 1962. Das erdoelfeld landau. *Abh. Geol. Baden-Württemberg* 4, 81–101.

- Schellschmidt, R., Clauser, C., 1996. The thermal regime of the Upper Rhine Graben and the anomaly at Soultz. *Zeitschrift für Angewandte Geologie* 42, 40–44.
- Schill, E., Genter, A., Cuenot, N., Kohl, T., 2017. Hydraulic performance history at the Soultz EGS reservoirs from stimulation and long-term circulation tests. *Geothermics* 70, 110–124. <http://dx.doi.org/10.1016/j.geothermics.2017.06.003>.
- Schindler, M., Baumgärtner, J., Gandy, T., Hauffe, P., Hettkamp, T., Menzek, H., Penzkofer, P., Teza, D., Wahl, G., Tischner, T., 2010. Successful hydraulic stimulation techniques for electric power production in the Upper Rhine Graben, Central Europe. In: *Proceedings of World Geothermal Congress 2010*. Bali, Indonesia.
- Schleicher, A.M., Warr, L.N., Kober, B., Laverret, E., Clauer, N., 2006. Episodic mineralization of hydrothermal illite in the Soultz-sous-Forêts granite (Upper Rhine Graben, France). *Contrib. Mineral. Petrol.* 152, 349–364. <http://dx.doi.org/10.1007/s00410-006-0110-7>.
- Schulte, T., Zimmermann, G., Vuataz, F.-D., Portier, S., Tischner, T., Junker, R., Jatho, R., Huenges, E., 2010. Enhancing Geothermal Reservoirs. In: *Geothermal Energy Systems – Exploration, Development, and Utilization*. Ernst Huenges, Weinheim, Germany, pp. 173–243.
- Schumacher, M.E., 2002. Upper Rhine Graben: role of preexisting structures during rift evolution. *Tectonics* 21. <http://dx.doi.org/10.1029/2001tc900022>. 6–1 to 6–17.
- Sittler, C., 1985. Les hydrocarbures d'Alsace dans le contexte historique et géodynamique du fossé Rhénan. *Bulletin des Centres de Recherches Elf Exploration Production* 9, 335–371.
- Smith, M.P., Savary, V., Yardley, B.W.D., Valley, J.W., Royer, J.J., Dubois, M., 1998. The evolution of the deep flow regime at Soultz-sous-Forêts, Rhine Graben, eastern France: evidence from a composite quartz vein. *J. Geophys. Res.* 103, 27223–27237. <http://dx.doi.org/10.1029/98JB02528>.
- Stober, I., Jodocy, M., 2009. Eigenschaften geothermischer Nutzhorizonte im abdenwürttembergischen und französischen Teil des Obberheingrabens. *Grundwasser – Zeitschrift der Fachsektion Hydrogeologie* 14, 127–137. <http://dx.doi.org/10.1007/s00767-009-0103-3>.
- Stussi, J.-M., Cheilletz, A., Royer, J.-J., Chèvremont, P., Gilbert, F., 2002. The hidden monzogranite of Soultz-sous-Forêts (Rhine Graben, France), mineralogy, petrology and genesis. *Géologie de la France* 1, 45–64.
- Traineau, H., Genter, A., Cautru, J.-P., Fabriol, H., Chèvremont, P., 1992. Petrography of the granite massif from drill cutting analysis and well log interpretation in the geothermal HDR borehole GPK-1 (Soultz, Alsace, France). In: Bresee, James C. (Ed.), *Geothermal Energy in Europe – The Soultz Hot Dry Rock Project*. Gordon and Breach Science Publishers, Montreux, Switzerland, pp. 1–29.
- Valley, B., 2007. *The Relation Between Natural Fracturing and Stress Heterogeneities in Deep-seated Crystalline Rocks at Soultz-sous-Forêts (France)*. PhD Thesis. Swiss Federal Institute of Technology, Zurich.
- Vernoux, J.-F., Genter, A., Razin, P., Vinchon, C., 1995. Geological and Petrophysical Parameters of a Deep Fractured Sandstone Formation as Applied to Geothermal Exploitation: EPS1 Borehole, Soultz-sous-Forêts, France (Open File No. BRGM/R 38622). BRGM, Orléans, France.
- Vidal, J., Genter, A., Schmittbuhl, J., 2015. How do permeable fractures in the Triassic sediments of Northern Alsace characterize the top of hydrothermal convective cells? Evidence from Soultz geothermal boreholes (France). *Geotherm. Energy J.* 3. <http://dx.doi.org/10.1186/s40517-015-0026-4>.
- Vidal, J., Genter, A., Chopin, F., Dalmais, E., 2016a. Natural fractures and permeability at the geothermal site Rittershoffen, France. In: *Proceedings of European Geothermal Congress 2016*. Strasbourg, France.
- Vidal, J., Genter, A., Schmittbuhl, J., 2016b. Pre- and post-stimulation characterization of geothermal well GRT-1, Rittershoffen, France: insights from acoustic image logs of hard fractured rock. *Geophys. J. Int.* 206, 845–860. <http://dx.doi.org/10.1093/gji/ggw181>.
- Vidal, J., Ulrich, M., Whitechurch, H., Genter, A., Schmittbuhl, J., Dalmais, E., Girard-Berthet, V., 2016c. Hydrothermal alteration of the hidden granite in the geothermal context of the Upper Rhine Graben. In: *Proceedings of Forty-First Workshop on Geothermal Reservoir Engineering*. Stanford University, California, USA.
- Vidal, J., Genter, A., Chopin, F., 2017a. Permeable fracture zones in the hard rocks of the geothermal reservoir at Rittershoffen, France. *J. Geophys. Res. Solid Earth* 122. <http://dx.doi.org/10.1002/2017JB014331>.
- Vidal, J., Patrier Mas, P., Genter, A., Beaufort, D., 2017b. Occurrences of clay minerals in permeable fracture zones in the granitic basement of geothermal wells at Rittershoffen, France. In: *Proceedings of Forty-Second Workshop on Geothermal Reservoir Engineering*. Stanford University, California, USA.
- Villemin, T., Bergerat, F., 1987. L'évolution structurale du Fosse rhénan au cours du Cénozoïque: un bilan de la déformation et des effets thermiques de l'extension. *Bulletin de la Société Géologique de France* 8, 245–255.
- Ziegler, P.A., 1990. *Geological Atlas of Western and Central Europe*, 2nd edition. Shell International Petroleum Mij B V, London, Great Britain.